

Modeling and control of flow problems by adaptation-based linear parameter varying models

Coşku KASNAKOĞLU

*Department of Electrical and Electronics Engineering,
TOBB University of Economics and Technology
06560 Ankara-TURKEY
e-mail: kasnakoglu@etu.edu.tr*

Abstract

In this paper a systematic modeling and control approach for flow problems is considered. A nonlinear Galerkin model is obtained from the partial differential equations (PDEs) describing the flow; and a Linear Parameter Varying (LPV) model is constructed to approximate the Galerkin model, where the parameter variation of the LPV model is controller by an adaptation mechanism. The LPV model is then treated as a surrogate on which the control design is carried out, where the parameter variations provide a range of uncertainty in which the control design must perform satisfactorily. It is shown that if certain conditions are met, then such a controller design will succeed when applied to the nonlinear Galerkin model. The ideas developed in the present paper are illustrated through a flow control example governed by the Navier-Stokes (NS) PDEs, where it is observed that a controller design based on the proposed approach is successful in achieving a desired regulation within the flow domain. In addition, it is seen that the LPV model can be used to predict certain robustness properties of the closed-loop system.

Key Words: *Flow control, Navier-Stokes, linear parameter varying (LPV) proper orthogonal decomposition (POD), Galerkin projection (GP), input separation (IS), adaptive control, robust control, disturbance rejection*

1. Introduction

The flow of fluids is a phenomenon observed everywhere in every aspect of life. The flow of air around the body of an airplane or automobile, water flow around the hull of a ship or submarine, the winds in the atmosphere, the waves in the oceans, the motion of water or petroleum through pipelines are all examples of this common and important concept. The ability to understand and have control over fluid flow is a topic of active research, the benefits of which include reducing fuel costs in vehicles and improving the effectiveness of industrial processes [1, 2]. Among numerous studies on flow control one finds research regarding flow control in aircrafts and airfoils [3, 4], control of channel flows [5, 6, 7, 8], control of turbulent boundary layers [9],

control of combustion instability [10], stabilization of bluff-body flow [11], control of cylinder wakes [12, 13, 14], control of cavity flows [15, 16, 17, 18, 19], optimal control of vortex shedding [20, 21] and control of fluid flow in capillaries [22, 23].

For the mathematical modeling of fluid flow, partial differential equations (PDEs) such as the Navier-Stokes (NS) and Burgers' equations are commonly used. While control design can be performed directly on these PDEs [24, 25, 26, 27, 28], it is preferable to obtain simplified models, using Proper Orthogonal Decomposition (POD) and Galerkin Projection (GP) methods [29, 30] together with input separation (IS) techniques [31, 32, 33, 34]. The resulting models are called *Galerkin models* and have been employed widely in applications, such as the control of cylinder wakes [12, 13, 14] and the control of cavity flows [15, 16, 17, 18, 19]. Despite their widespread use in flow control applications, Galerkin models are nonlinear, thus special and complicated nonlinear control theoretic methods must be utilized for analysis and control design. One possibility towards further simplification is to use linearization; however, this will limit the analysis and control design to a single operating condition, which is unacceptable for many problems. A less restrictive alternative is to utilize Linear Parameter Varying (LPV) models to represent the flow process. LPV models have a linear structure, but some of the system parameters may vary with time. Such models have been used in the control of steam generators in nuclear power plants [35], robust control of combustion instability [36], control of high-performance turbofan engines [37], identification and gain-scheduled control of rotating stall and surge [38], control of driven cavities [39], control of structural dynamics with aerothermoelastic effects [40], and gain-scheduled velocity/force control of electrohydraulic servo systems [41].

While LPV models are less restrictive compared to linearization based models and may provide an attractive alternative to dealing directly with nonlinear Galerkin models, the lack of standard methodologies to obtain LPV models for flow control processes is a major difficulty. In this work we start from a nonlinear Galerkin model and develop a systematic approach to represent it with an LPV model, through the use of techniques based on adaptation [42, 43, 44, 45, 46]. The idea is to first utilize POD/GP/IS techniques to obtain a reduced order nonlinear Galerkin model representing the flow, transform this model into a form that is linear in its parameters (Section 2), and build an adaptation mechanism to yield an LPV model approximating the nonlinear Galerkin model (Section 3). The usefulness and potential of such an approach for control design is illustrated by designing an \mathcal{H}_∞ controller on the LPV model (Section 4), and showing that this controller will also succeed when applied to the nonlinear Galerkin model, provided that certain conditions are satisfied (Section 5). The ideas developed in the paper are demonstrated on a flow control example, where the fluid dynamics are governed by the Navier-Stokes PDEs (Section 7). The paper is finalized with conclusions, discussions and ideas for future work (Section 8).

2. Modeling of the flow process

The first step is to obtain a dynamical model for the flow process that is amenable to the design of an adaptation mechanism and a controller. Let \mathbb{H} be a real Hilbert space with inner product $\langle \cdot, \cdot \rangle : \mathbb{H} \times \mathbb{H} \rightarrow \mathbb{R}$. Let $q : \Omega \times \mathbb{R}_+ \rightarrow \mathbb{R}$, $q(\cdot, \cdot, t) \in \mathbb{H}$, $q(x, y, \cdot) \in \mathcal{C}^k$ and $k \in \mathbb{N}$. Here, $t \in \mathbb{R}_+$ is the temporal variable, $\Omega \subset \mathbb{R}^2$ is the flow domain and $x \in \Omega$ is the spatial variable. The evolution of the flow field is governed by a partial

differential equation (PDE) of the form

$$\dot{q} = X(q), \quad (1)$$

where the operator $X : \mathbb{H} \rightarrow \mathbb{H}$ includes spatial derivatives. Equation (1) is subject to the initial condition

$$q(x, 0) = q_{\text{init}}(x), \quad (2)$$

where $q_{\text{init}} \in \mathbb{H}$, and subject to the boundary conditions

$$(B_i(q, u))(x, t) = b_i(x, t), \quad i = 1 \dots n_b \quad (3)$$

where $x \in \partial\Omega$, $t \in \mathbb{R}_+$, $B_i : \mathbb{H} \times \mathcal{C}^k \rightarrow \mathbb{H}$, $b_i \in \mathbb{H}$, and $n_b \in \mathbb{N}$. The control input $u \in \mathbb{R}$ acts through the boundary conditions. The operator B may include spatial derivatives.

The task considered in this section is to transform the infinite order PDE described in (1)–(3), into a form that is suitable for adaptation and control design, i.e. a finite system of ordinary differential equations which are linear in the parameters θ and to which u enters explicitly. This means obtaining an ordinary differential equation system of the form

$$\dot{a} = f_\theta(a, u) = \Phi(a, u)\theta, \quad a(0) = a_0 \quad (4)$$

where $f_\theta : \mathbb{R}^n \times \mathbb{R} \rightarrow \mathbb{R}^n$, $\theta \in \mathbb{R}^p$, $a \in \mathbb{R}^n$ and $p, n \in \mathbb{N}$ in such a way that (4) represents the original PDE (1)–(3) in some sense. The approach that will be utilized for this purpose is based on a POD/GP/IS method [34, 47, 48], a brief review of which is provided next.

Define $q_k(x, y) := q(x, t_k)$ as the *snapshot* of the flow taken at time t_k and let $\{q_k\}_{k=1}^{n_s} \subset \mathbb{H}$ be an ensemble of $n_s \in \mathbb{N}$ snapshots collected at times $\{t_k\}_{k=1}^{n_s}$. Let $q_0 := E[q_j]$, where E is a linear averaging operation $E[q_j] = n_s^{-1} \sum_{j=1}^{n_s} w_j q_j$ for given weights $w_j > 0$. From the snapshots $\{q_k\}_1^{n_s}$, the POD procedure is used to obtain a set of *POD modes* $\{\phi_i\}_1^n \subset \mathbb{H}$ and a set of *modal coefficients* $\{a_i\}_1^n \subset \mathbb{R}$ so that¹

$$q(x, t) \approx q_0(x) + \sum_{i=1}^n a_i(t) \phi_i(x). \quad (5)$$

A dynamical system that approximates the flow dynamics can be obtained by Galerkin projection as $\dot{r} = X_S(r)$, where $r := q_0 + \sum_{i=1}^n a_j \phi_j \in S$, and $S := q_0 + \text{span}\{\phi_1, \dots, \phi_n\}$. Simplification yields the set of nonlinear ODEs

$$\dot{a}_k = \langle X(r), \phi_k \rangle, \quad k = 1 \dots n. \quad (6)$$

Note that at this stage, the effect of the actuation is still embedded in the coefficients of the Galerkin system and does not appear explicitly in (6). Therefore an input separation (IS) method based on expanding the flow field in terms of *baseline POD modes* and *actuation modes* will be utilized to separate the effect of the input from the Galerkin system coefficients and make it appear as a stand-alone term. The baseline modes ϕ_i are extracted from the unactuated flow using a standard POD procedure as in (5). Next, an *innovation* flow field is defined as $\tilde{q}(x, t) := q(x, y, t) - P_S q(x, t)$, where $S := q_0 + \text{span}\{\phi_i\}$ and P_S is the projection operator onto S . Forced flow snapshots are projected onto the span of the baseline (unactuated) POD modes to obtain the

¹Whenever convenient, we will use Einstein notation to omit summation signs and write $q(x, t) \approx q_0(x) + a_i(t) \phi_i(x)$ in place of (5).

portion of the controlled flow that is recovered by S , whereas the innovation yields the information which is not captured by S and is due to the effect of the actuation. Next, the actuation modes are built from the innovations as follows. For simplicity assume that we only use a single scalar input u . We then consider an expansion of the form

$$q(x, t) \approx q_0(x) + \sum_{i=1}^n a_i(t)\phi_i(x) + \psi(x)u(t), \tag{7}$$

where the actuation mode ψ is to be chosen so as to minimize the energy not captured by such an expansion. An optimization problem on the Hilbert space \mathbb{H} can be defined as finding

$$\psi^* = \arg \min_{\psi \in \mathbb{H}} J(\psi), \tag{8}$$

where $J(\psi) := E [\|\tilde{q}_k - u_k\psi\|^2]$. The element $\psi^* \in \mathbb{H}$ will be chosen as the actuation mode. The squared norm of the velocity represents the energy contained in the flow. Therefore, among all augmented POD expansions in the form given in (7), where *the input u directly appears as the coefficient of ψ* , the choice $\psi = \psi^*$ is optimal, in the sense that the energy not captured by this expansion achieves its minimum for $\psi = \psi^*$. It was shown in [34] that ψ^* solving the optimization problem (8) can be obtained as

$$\psi^* = \frac{E [u_k \tilde{q}_k]}{E [u_k^2]}. \tag{9}$$

The Galerkin model is then obtained by substituting (7) into (6), which gives a dynamics of the form

$$\dot{a}_i = C_i + L_{ik}a_k + L_{in,i}u + Q_{ijk}a_k a_j + Q_{ain,ik}a_k u + Q_{in}u^2 \tag{10}$$

for $i = 1, \dots, n$. Equation (10) can be expressed compactly as

$$\dot{a} = C + La + L_{in}u + Q(a, a) + Q_{ain}(a, u) + Q_{in}(u, u). \tag{11}$$

Equation (11) can be simplified further by eliminating the constant term C if the system has an equilibrium at $a = a_d$. In this case it holds that

$$C + La_d + Q(a_d, a_d) = 0. \tag{12}$$

One can then define a shift of coordinates $\tilde{a} = a - a_d$, which yields

$$\dot{\tilde{a}} = \tilde{L}\tilde{a} + Q(\tilde{a}, \tilde{a}) + \tilde{L}_{in}u + Q_{in}(u, u) + Q_{ain}(\tilde{a}, u), \tag{13}$$

where

$$\begin{aligned} \tilde{L} &= L + Q(\cdot, a_d) + Q(a_d, \cdot) \\ \tilde{L}_{in} &= L_{in} + Q_{ain}(a_d, \cdot). \end{aligned}$$

Note that system (13) has an equilibrium at $\tilde{a} = 0$, which corresponds the equilibrium state $a = a_d$.

While the system in (13) is nonlinear in its state a and its input u , it is linear in its parameter values contained in \tilde{L} , Q , \tilde{L}_{in} , Q_{in} and Q_{ain} , since there are no terms involving the multiplication of two parameter

values. To write the dynamics in a form where this linear dependence is apparent, let us first build the parameter vector θ as

$$\theta := \text{col} \left\{ \tilde{L}(\cdot), \tilde{L}_{\text{in}}(\cdot), Q(\cdot), Q_{\text{in}}(\cdot), Q_{\text{ain}}(\cdot) \right\}, \quad (14)$$

where col stands for column vector, i.e. $\text{col}\{x_1, x_2, \dots, x_n\} = [x_1^T \ x_2^T \ \dots \ x_n^T]^T$, and $\tilde{L}(\cdot)$ denotes the column vector formed by stacking all elements of L on top of each other, e.g.

$$\tilde{L}(\cdot) := \text{col} \left\{ \tilde{L}_{11}, \tilde{L}_{21}, \dots, \tilde{L}_{n-1,n}, \tilde{L}_{nn} \right\}. \quad (15)$$

The definitions for $\tilde{L}_{\text{in}}(\cdot)$, $Q(\cdot)$, $Q_{\text{in}}(\cdot)$ and $Q_{\text{ain}}(\cdot)$ follow similarly. One can then define $\Phi : \mathbb{R}^n \times \mathbb{R}^m \rightarrow \mathbb{R}^n \times \mathbb{R}^p$ such that

$$\dot{\tilde{a}} = \Phi(\tilde{a}, u)\theta, \quad (16)$$

where $\Phi(\tilde{a}, u)$ is a $n \times p$ matrix with elements $\{\Phi(\tilde{a}, u)_{ij} \mid i = 1, \dots, n, j = 1, \dots, p\}$ such that $\Phi(\tilde{a}, u)_{ij}$; the element at row i and column j , corresponds to the contribution of the j th parameter in θ to the i th state of \tilde{a} . For instance, from (14) one sees that the second parameter in θ is the second parameter of \tilde{L} , which from (15) is seen to be \tilde{L}_{21} . Also, it can be seen that the second element in the state vector $\tilde{a} = \text{col}\{\tilde{a}_1, \tilde{a}_2, \tilde{a}_3, \dots, \tilde{a}_n\}$ is \tilde{a}_2 . Looking at (13), if we highlight the portion of the dynamics of \tilde{a}_2 where the term L_{21} appears,

$$\dot{\tilde{a}}_2 = \dots + L_{21}\tilde{a}_1 + \dots,$$

which implies that $\Phi(\tilde{a}, u)_{22} = \tilde{a}_1$. Other elements of $\Phi(\tilde{a}, u)$ can be constructed similarly so as to write the system in the desired linear parameter form shown in (16).

From now on we will drop the tildes in (16) to simplify the notation and write

$$\dot{a} = \Phi(a, u)\theta. \quad (17)$$

It will be implicitly understood that the system has already been shifted by the equilibrium value.

3. Approximating the galerkin system with an adaptation based linear parameter varying model

The goal in this section is to design a linear parameter varying (LPV) system of the form

$$\dot{\hat{a}}(t) = \hat{L}(t)\hat{a}(t) + \hat{L}_{\text{in}}(t)u(t) + \hat{L}_{\text{err}}(t)(\hat{a}(t) - a(t)), \quad (18)$$

which approximates the system in (17); that is, if $e_d := \hat{a} - a$, then e_d should be kept “small,” where smallness can be in terms of amplitude (keeping $\|e_d\|_\infty$ small), energy (keeping $\|e_d\|_2$ small) or any other means to quantify e_d . The variation of \hat{L} , \hat{L}_{in} and \hat{L}_{err} with time will be controlled through an adaptation mechanism. The states \hat{a} of the LPV model above will be referred to as the *adapted states* or as the *reconstructed states*.

First, note that the Galerkin system in (17) can be written as

$$\begin{aligned} \dot{a} &= \Phi(a, u)\theta \\ \dot{a} &= \Phi_L(a, u)\theta_L + \Phi_N(a, u)\theta_N \\ \dot{a} &= La + L_{in}u + Q(a, a) + Q_{ain}(a, u) + Q_{in}(u, u), \end{aligned} \tag{19}$$

where we have split the linear and nonlinear parts of the Galerkin system as

$$\begin{aligned} \Phi_L(a, u)\theta_L &:= La + L_{in}u \\ \Phi_N(a, u)\theta_N &:= Q(a, a) + Q_{ain}(a, u) + Q_{in}(u, u). \end{aligned} \tag{20}$$

We consider a linear model of the form

$$\dot{\hat{a}} = \Phi_L(a, u)\hat{\theta}_L - ke_d = \hat{L}a + \hat{L}_{in}u - ke_d \tag{21}$$

whose parameter vector $\hat{\theta}_L$ will be modified by an adaptation mechanism to match the Galerkin system (19). For later reference we also state the dynamics of e_d as

$$\dot{e}_d = \dot{\hat{a}} - \dot{a} = \Phi_L(a, u)\hat{\theta}_L - ke_d - \Phi_L(a, u)\theta_L - \Phi_N(a, u)\theta_N. \tag{22}$$

The adaptation mechanism considered is of the following form

$$\dot{\hat{\theta}}_L = -\Phi_L^T(a, u)e_d - \Upsilon(\hat{\theta}_L, a, u) - \Psi(\hat{\theta}_L), \tag{23}$$

where $\Upsilon(\hat{\theta}_L, a, u) := \hat{\theta}_L^* \|\text{col}(a, u)\|^2 + \hat{\theta}_L^* \|\text{col}(a, u)\|^4$,

$$\hat{\theta}_L^* := \begin{cases} 0, & \hat{\theta}_L = 0; \\ \hat{\theta}_L / \|\hat{\theta}_L\|^2, & \hat{\theta}_L \neq 0, \end{cases} \tag{24}$$

$$\Psi(\hat{\theta}_L) := \begin{cases} k_\epsilon \hat{\theta}_L, & \|\hat{\theta}_L\| < b; \\ k_d \hat{\theta}_L, & \|\hat{\theta}_L\| \geq b, \end{cases} \tag{25}$$

and $k, k_\epsilon, k_d, b \in \mathbb{R}_+$ are the adaptation constants. The constant k must be set high enough so that the adaptation error e_d can be kept to a reasonable value, but excessively high values of k may lead to undesirable overcorrection and oscillatory behavior. The constants k_ϵ, k_d, b are related to the term $\Psi(\hat{\theta}_L)$, which adds dissipation to the adaptation dynamics (23) and ensures the boundedness of the parameter trajectories. The value of k_ϵ is set to a small value so that for $\|\hat{\theta}_L\| < b$ the effect of the term $\Psi(\hat{\theta}_L)$ to the adaptation dynamics is negligible. The value of k_d is set to a large value so that for $\|\hat{\theta}_L\| \geq b$, the dissipation term dominates the dynamics, and hence prevents the unboundedness of the parameter trajectories. The value b determines the range in which the parameter vector $\hat{\theta}_L$ can vary freely, and beyond which the dissipative term $\Psi(\hat{\theta}_L)$ will interfere. This constant is determined in a two-step procedure: First b is set to a very large value, so that the dissipative term $\Psi(\hat{\theta}_L)$ practically has no effect on the dynamics. The Galerkin system system and adaptation scheme are run with a rich variety of inputs including constant values, sine waves, square waves, chirp signals etc., covering the amplitude and frequency ranges of interest. From these experiments the range Θ in which

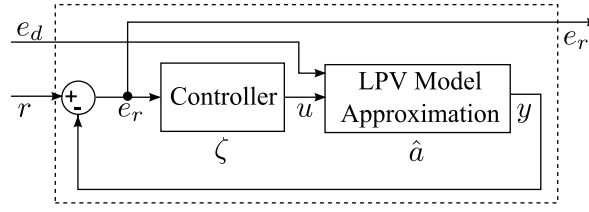


Figure 1. Block diagram using a LPV model to approximate the nonlinear Galerkin model, for a reference tracking problem.

the parameter vector $\hat{\theta}_L$ varies is determined. The parameter b is then set to a certain percentage of $\|\Theta\|$, e.g. $b = 0.9\|\Theta\|$. With this value of b , the term $\Psi(\hat{\theta}_L)$ starts providing dissipation to the adaptation dynamics as $\hat{\theta}_L$ begins to approach the boundaries of the allowable range Θ , preventing unbounded growth of the parameter vector.

4. Control design

Consider the Galerkin system given by the state dynamics (19). By using the adaptation scheme (23) with properly selected values of its constants, the error $e_d = \hat{a} - a$ can be made to remain bounded and small. This means that the state trajectories of the system (21) will remain close to those of the Galerkin system (19). We will provide a justification for this statement shortly, but for now, let us just assume that this is the case. Then, if (21) is rearranged as

$$\begin{aligned}\dot{\hat{a}} &= \hat{L}a + \hat{L}_{\text{in}}u - ke_d \\ \dot{\hat{a}} &= \hat{L}(\hat{a} - e_d) + \hat{L}_{\text{in}}u - ke_d \\ \dot{\hat{a}} &= \hat{L}\hat{a} + \hat{L}_{\text{in}}u + \hat{L}_{\text{err}}e_d,\end{aligned}\tag{26}$$

where $\hat{L}_{\text{err}} = -(\hat{L} + kI)$, one can then observe that (26) is of the same form as (18). Thus, if the signal e_d is small, one can regard system (21) as a linear parameter-varying system that approximates the original system, with the signal e_d entering as an external disturbance. With this interpretation, the controller design can be performed on the LPV system (26), instead of the nonlinear Galerkin model (19). In this section we will consider one such design, an illustration of which is given in Figure 1. The objective of the control design is to track a given reference signal r , while limiting the effect of the disturbance signal e_d on the tracking error $e_r := y - r$. For simplicity, the output of interest (y) is assumed to be a linear expression in terms of the Galerkin system state a and input u

$$y = L_{\text{out}}a + L_{\text{out},\text{in}}u.\tag{27}$$

Expressing the output in terms of the adapted state \hat{a} gives

$$\begin{aligned}y &= L_{\text{out}}(\hat{a} - e_d) + L_{\text{out},\text{in}} \\ &= L_{\text{out}}\hat{a} + L_{\text{out},\text{in}}u + L_{\text{out},\text{err}}e_d,\end{aligned}\tag{28}$$

where $L_{\text{out,err}} = -L_{\text{out}}$. Augmenting with the state dynamics (26) yields the system

$$\dot{\hat{a}} = \hat{L}\hat{a} + \hat{L}_{\text{in}}u + \hat{L}_{\text{err}}e_d \tag{29}$$

$$y = L_{\text{out}}\hat{a} + L_{\text{out,in}}u + L_{\text{out,err}}e_d. \tag{30}$$

The task to be achieved can be stated as an \mathcal{H}_∞ control problem of determining a stabilizing controller for this system such that the \mathcal{L}_2 gain from $\|\text{col}(e_d, r)\|_2$ to $\|e_r\|_2$ is less than a desired value γ_{max} . In other words,

$$\|e_r\|_2 < \gamma \|\text{col}(e_d, r)\|_2 \tag{31}$$

for all $\hat{\theta}_L \in \Theta$, where $\gamma < \gamma_{\text{max}}$; here γ is called the \mathcal{H}_∞ cost. This problem has been studied extensively for linear systems and efficient solution methods are available, including the cases when there is uncertainty/time-variation on system parameters, and including the situations when one must impose constraints on the system poles [49, 50, 51]. Hence the controller design can be carried out in a straightforward manner using these available methods, most of which are available as built-in routines in common scientific computing software (e.g. MATLAB).

5. Analysis of the closed-loop system

The main question at this point is whether the controller designed on the system (29)–(30) will perform satisfactorily when applied to the nonlinear Galerkin model (19) representing the flow process. The theorem below answers this question to the affirmative, provided that some conditions are satisfied.

Theorem 5.1 *Assume that there exists a linear dynamical controller K*

$$\dot{\zeta} = A_K\zeta + B_Ke_r \tag{32}$$

$$u = C_K\zeta + D_Ke_r \tag{33}$$

for the LPV system (29)–(30) that achieves a finite \mathcal{L}_2 gain of γ from $\text{col}(e_d, r)$ to e_r for the closed-loop system (see Figure 1), for all $\hat{\theta}_L \in \Theta$, such that γ satisfies

$$0 < \gamma^2 < k - \frac{k_6^2}{2} - \frac{k_7^2}{2} - 1, \tag{34}$$

where

$$k_6 := \max \{ \|L\|, \|L_{\text{in}}\| \} \tag{35}$$

$$k_7 := \max \left\{ \|Q\| + \frac{1}{2}\|Q_{\text{ain}}\|, \|Q_{\text{in}}\| + \frac{1}{2}\|Q_{\text{ain}}\| \right\}. \tag{36}$$

Then, when the controller K in (32)–(33) is applied to the nonlinear Galerkin system with state dynamics (19) and output (27), it holds that:

1. If r is bounded, then all trajectories of the closed-loop system are bounded.

2. The closed-loop system has finite \mathcal{L}_2 gain from r to e_r , and from r to e_d . Specifically,

$$\|e_r\|_2 \leq \gamma \|r\|_2, \tag{37}$$

$$\|e_d\|_2 \leq \left(\frac{\gamma^2}{k - \frac{k_a^2}{2} - \frac{k_z^2}{2} - \gamma^2} \right)^{\frac{1}{2}} \|r\|_2. \tag{38}$$

Proof See Appendix A. □

From the above theorem one can see that, for the controller designed on the LPV system to be successful on the nonlinear Galerkin model, the cost γ must be below a certain value, namely $(k - \frac{k_a^2}{2} - \frac{k_z^2}{2} - 1)^{\frac{1}{2}}$. Note that the term inside the square root must be positive, so this condition implicitly poses a restriction on the adaptation gain k in that $k < \frac{k_a^2}{2} + \frac{k_z^2}{2} + 1$ must hold. If (34) is satisfied then from (37) and (38) one can see that the reference signal r is able to energize the tracking error e_r , and the adaptation error e_d by only a limited amount, determined by the \mathcal{L}_2 gains in (37) and (38). Lower values of the cost γ will reduce the tracking error e_r , as well as the the adaptation error e_d . Higher values of the adaptation gain k have no effect on e_r , but seem to reduce e_d .

Remark 5.1 *At this point we remark that the main focus of the paper is to present a systematic procedure to obtain LPV models for Galerkin systems using adaptation mechanisms. Once this model is at hand, we leave it to the designer to chose from the various options available as to how the controller can be obtained. A couple of these possibilities include (but are not limited to):*

1. *One can carry out a parametric controller design; i.e., one can build an LPV controller which utilizes the parameter vector $\hat{\theta}_L$ in real-time, using several established methods in literature such as the self-scheduled \mathcal{H}_∞ controller design method described in [51]. In this method one first solves a set of LMIs at the vertices of the polytope in which the parameter vector $\hat{\theta}_L$ varies, which yields the controller matrices at these vertices. During closed-loop operation, the controller matrices are recomputed at every time instant t by utilizing a convex decomposition based on the current value of $\hat{\theta}_L(t)$.*
2. *One can carry out a classical robust control design approach. In this approach the parameter vector $\hat{\theta}_L$ is not utilized online, but the LPV model built is preprocessed to obtain: i) a range of uncertainty Θ in which the parameter $\hat{\theta}_L$ will vary, and ii) a nominal model. For the former one can apply a number of diverse input signals (e.g. sinusoids, square waves, white noise, etc.) to the system and the record the trajectories of the parameter vector $\hat{\theta}_L$, the upper and lower bounds of which will determine the range Θ . For the latter, i.e. to obtain a nominal model, one can select the centroid of the box Θ and instantiate the LPV model at this parameter value. This will yield a nominal LTI model that is independent of the parameter $\hat{\theta}_L$. Once the nominal model and the range for $\hat{\theta}_L$ is known, we are done with the LPV model; unlike the LPV controller design approach mentioned in the item above, the parameter $\hat{\theta}_L$ is not used in real-time by the controller. Having obtained a nominal LTI model and a knowledge of the uncertainty on this model, one can employ standard robust control approaches to obtain the controller and evaluate it in this range of uncertainty.*

As indicated earlier, the main focus of this paper is modeling, so we do not dictate a particular controller design strategy as long as the resulting controller satisfies the conditions of Theorem 5.1. However, for the sake of completeness, in the case study example given in Section 7, we adopt the second approach above since it is relatively easy to implement using the readily available routines in MATLAB. In particular we employ an \mathcal{H}_∞ design with pole placement constraints, where the idea is to solve a trace minimization problem subject to LMI constraints to guarantee a certain \mathcal{H}_∞ performance while at the same time assuring that the systems poles will be clustered in a desired region. Full details of this method can be found in [51] and it is readily implemented in MATLAB by the function `h2hinfsyn`.

6. Summary of steps

Below we summarize the steps for the modeling and the controller design approach considered in the paper for flow control problems:

1. Obtain a Galerkin model from the Navier-Stokes PDEs using POD/GP/IS.
2. Set up the LPV model and the adaptation mechanism.
3. Apply a number of diverse input signals to the system and determine the parameter range Θ for the LPV model.
4. Design an \mathcal{H}_∞ controller on the LPV model, such that the controller archives a desired performance γ , where γ satisfies the criteria in Theorem 5.1.
5. Apply the controller to the nonlinear Galerkin model, simulate and evaluate the results.
6. Apply the controller to the Navier Stokes PDEs, perform computational fluid dynamics (CFD) simulations and evaluate the results.

In the next section we illustrate the application of these steps to a sample flow control problem.

7. Example: Boundary control of 2D incompressible navier-stokes equations on a square domain

7.1. Problem description

We consider the two-dimensional, incompressible, nondimensionalized Navier-Stokes equation

$$\frac{\partial q}{\partial t} + (q \cdot \nabla)q = -\nabla p + \frac{1}{Re} \nabla^2 q \quad (39)$$

$$\nabla \cdot q = 0, \quad (40)$$

where Re is a constant value called the *Reynolds number*. Let $p(x, y, t) \in \mathbb{R}$ denote the pressure, and $q(x, y, t) = (q_u(x, y, t) \ q_v(x, y, t)) \in \mathbb{R}^2$ denote the flow velocity, where q_u and q_v are the components in

the longitudinal and latitudinal directions, respectively. In the given coordinates, (39) reads as

$$\begin{aligned}\frac{\partial q_u}{\partial t} + \frac{\partial q_u}{\partial x} q_u + \frac{\partial q_u}{\partial y} q_v &= -\frac{\partial p}{\partial x} + \frac{1}{Re} \left(\frac{\partial^2 q_u}{\partial x^2} + \frac{\partial^2 q_u}{\partial y^2} \right) \\ \frac{\partial q_v}{\partial t} + \frac{\partial q_v}{\partial x} q_u + \frac{\partial q_v}{\partial y} q_v &= -\frac{\partial p}{\partial y} + \frac{1}{Re} \left(\frac{\partial^2 q_v}{\partial x^2} + \frac{\partial^2 q_v}{\partial y^2} \right).\end{aligned}\quad (41)$$

For our example we set $Re = 10$, and the spatial domain is defined as $\Omega = [0, 1] \times [0, 1]$. The initial conditions are $q_u(x, y, 0) = q_v(x, y, 0) = 0$ and the boundary conditions are

$$\begin{aligned}q_u(x, 0, t) &= 1, \quad q_v(x, 0, t) = 0 \\ q_u(x, 1, t) &= 1, \quad q_v(x, 1, t) = 0 \\ \frac{\partial q_u}{\partial x}(0, y, t) &= 0, \quad q_v(0, y, t) = 0 \\ q_u(1, y, t) &= \begin{cases} 0, & y \in [0, 0.42); \\ u(t), & y \in [0.42, 0.58]; \\ 0, & y \in (0.58, 1]. \end{cases} \\ q_v(1, y, t) &= 0,\end{aligned}$$

where $u \in \mathbb{R}$ is the control input. For this example, we shall define the control task as regulating the longitudinal speed at a given point $(x_c, y_c) \in \Omega$. In other words, if the system output y is defined as

$$y(t) = q_u(x_c, y_c, t), \quad (42)$$

and a reference signal $r : t \mapsto r(t)$ is given, then the goal is to achieve $y \rightarrow r$.

7.2. Modeling of the flow process

As noted in Section 2, the first task is to collect snapshots from the unforced response of the system, using which the baseline POD expansion is obtained. The number of modes is selected as $n = 3$, which is a good compromise between the amount of energy captured and the complexity of the reduced-order model. The actuation mode ψ is obtained using snapshots from operation under a chirp signal input. Next one uses GP to obtain a Galerkin of the form (11) for system (39)–(40), where C , L , L_{in} , Q , Q_{in} and Q_{ain} are as given in Appendix B. To obtain the system output, note from (42) and (5) that

$$\begin{aligned}y(t) &= q_{0u}(x_c, y_c) + \sum_{i=1}^n a_i(t) \phi_{i,u}(x_c, y_c) + u(t) \psi_u(x_c, y_c) \\ y &= q_{0u}(x_c, y_c) + L_{\text{out}} a + L_{\text{out}, \text{in}} u\end{aligned}\quad (43)$$

where $L_{\text{out}} := [\phi_{1,u}(x_c, y_c) \ \phi_{2,u}(x_c, y_c) \ \phi_{3,u}(x_c, y_c)] \in \mathbb{R}^{1 \times 3}$ and $L_{\text{out}, \text{in}} := \psi_u(x_c, y_c) \in \mathbb{R}$. Next, the Galerkin model is shifted coordinates, which results in a model of the form (13). This system has an equilibrium at $\tilde{a} = 0$, or equivalently $a = a_d$. Writing the system output (43) in shifted coordinates, we get

$$y = q_{0u}(x_c, y_c) + L_{\text{out}} \tilde{a} + L_{\text{out}} a_d + L_{\text{out}, \text{in}} u. \quad (44)$$

Since $q_{0u}(x_c, y_c) \in \mathbb{R}$ and $L_{out}a_d \in \mathbb{R}$ are constants, one can redefine the system output as $\tilde{y} = y - q_{0u}(x_c, y_c) - L_{out}a_d$ so that

$$\tilde{y} = L_{out}\tilde{a} + L_{out,in}u. \tag{45}$$

Augmenting the shifted Galerkin system with this output yields the system to be controlled

$$\dot{a} = La + Q(a, a) + L_{in}u + Q_{in}(u, u) + Q_{ain}(a, u) \tag{46}$$

$$y = L_{out}a + L_{out,in}u, \tag{47}$$

where the tildes have been dropped from both equations to simplify the notation.

7.3. Building an adaptation scheme to obtain the LPV model

For the adaptation process we consider the dynamics

$$\dot{\hat{a}} = \hat{L}a + \hat{L}_{in}u - ke,$$

or equivalently

$$\dot{\hat{a}} = \hat{L}\hat{a} + \hat{L}_{in}u - (\hat{L} + kI)e, \tag{48}$$

where $e := \hat{a} - a$, $\hat{L} \in \mathbb{R}^{3 \times 3}$, $\hat{L}_{in} \in \mathbb{R}^{3 \times 1}$, and the elements of \hat{L} and \hat{L}_{in} constitute the parameter vector $\hat{\theta}_L$. Normally $\hat{\theta}_L$ would contain $3 \times 3 + 3 \times 1 = 12$ elements to be estimated; however this would require that the adaptation law be a 12th order system, which is quite high order. To reduce the number of parameters we utilize the fact that for the problem under consideration, the eigenvalues of matrix L actually turn out to be of the form

$$\text{spec}(L) = \{\lambda_1, \lambda_2, \lambda_3\}, \tag{49}$$

where $\lambda_1, \lambda_2, \lambda_3 \in \mathbb{R}$. By applying a non-singular transformation $\bar{a} := Ta$, one can transform system (13) into modal form

$$\dot{\bar{a}} = \bar{L}\bar{a} + \bar{Q}(\bar{a}, \bar{a}) + \bar{L}_{in}u + \bar{Q}_{in}(u, u) + \bar{Q}_{ain}(\bar{a}, u) \tag{50}$$

where

$$\bar{L} = \begin{bmatrix} \lambda_1 & 0 & 0 \\ 0 & \lambda_2 & 0 \\ 0 & 0 & \lambda_3 \end{bmatrix}, \quad \bar{L}_{in} = \begin{bmatrix} b_1 \\ b_2 \\ b_3 \end{bmatrix}, \tag{51}$$

and \bar{Q} , \bar{Q}_{in} , and \bar{Q}_{ain} are quadratic functions in their elements.² With the transformation into modal form (50), the number of parameters to be estimated is reduced from 12 to 6, namely $\lambda_1, \lambda_2, \lambda_3, b_1, b_2$ and b_3 . As

²Note that fixing the eigenvalue spectrum as in (49) does not cause loss of generality. If the spectrum were different, one would simply transform into the modal form based on this structure and obtain the \bar{L} matrix accordingly. For instance if we had $\text{spec}(L) = \{\sigma + \omega, \sigma - \omega, \lambda\}$ this would result in

$$\bar{L} = \begin{bmatrix} \sigma & -\omega & 0 \\ \omega & \sigma & 0 \\ 0 & 0 & \lambda \end{bmatrix}$$

and the parameters to be estimated would be σ, ω and λ .

to the outputs of the system, we have that

$$\begin{aligned} y &= L_{\text{out}}a + L_{\text{out},\text{in}}u \\ &= L_{\text{out}}T^{-1}\bar{a} + L_{\text{out},\text{in}}u \\ &= \bar{L}_{\text{out}}\bar{a} + L_{\text{out},\text{in}}u \end{aligned}$$

where $\bar{L}_{\text{out}} := L_{\text{out}}T^{-1}$. From now on we shall drop the bars above the variables for the sake of simplicity and write the system simply as

$$\dot{a} = La + Q(a, a) + L_{\text{in}}u + Q_{\text{in}}(u, u) + Q_{\text{ain}}(a, u) \quad (52)$$

$$y = L_{\text{out}}a + L_{\text{out},\text{in}}u, \quad (53)$$

where L and L_{in} are as in (51); it will be implicitly understood that the system has been transformed into the modal form. We define the parameter vector as $\hat{\theta}_L := [\hat{\lambda}_1 \ \hat{\lambda}_2 \ \hat{\lambda}_3 \ \hat{b}_1 \ \hat{b}_2 \ \hat{b}_3]^T$, the individual elements of the state vector as $a := [a_1 \ a_2 \ a_3]^T$, and $\Phi_L(a, u)$ as

$$\Phi_L(a, u) := \begin{bmatrix} a_1 & 0 & 0 & u & 0 & 0 \\ 0 & a_2 & 0 & 0 & u & 0 \\ 0 & 0 & a_3 & 0 & 0 & u \end{bmatrix}.$$

With these definitions, the parameter adaptation mechanism (23) and the LPV model of the form (29)–(30) can be set up. Recall that the main goal of the adaptation mechanism is to provide an estimate for the range Θ in which the parameters of the LPV system vary. For this purpose, we apply numerous test signals of various types to the Galerkin system including ramp functions, sine functions, chirp functions, square waves and white noise, and record the values assumed by the parameters under these excitation signals. Observing the range in which the parameter values vary with these excitations, the range Θ such that $\hat{\theta}_L \in \Theta$ is chosen to be the 6-dimensional box

$$\begin{aligned} \Theta = \{ \hat{\theta}_L \in \mathbb{R}^6 : & -285.28 < \hat{\lambda}_1 < -163.20, -10.53 < \hat{\lambda}_2 < -8.02, -67.11 < \hat{\lambda}_3 < -27.72, \\ & -27.87 < \hat{b}_1 < -3.65, -5.45 < \hat{b}_2 < -0.24, -6.08 < \hat{b}_3 < -1.83 \}. \end{aligned} \quad (54)$$

The constants used for the adaptation mechanism are $k = 1000$, $k_\epsilon = 10^{-3}$, $k_d = 100$ and $b = 188.61$.

7.4. Controller design and evaluation

Once the range Θ for the parameter vector is obtained as in (54), control design is performed on the approximate LPV model (29)–(30) using standard \mathcal{H}_∞ design techniques by the help of MATLAB Robust Control Toolbox. Pole placement constraints were also imposed on the design to achieve a settling time less than one seconds for the closed-loop system.³ The resulting controller K is

$$\dot{\zeta} = \begin{bmatrix} 0 & 11.088 & 27.195 \\ 0 & -19.74 & 33.546 \\ 0 & 0 & -92.577 \end{bmatrix} \zeta + \begin{bmatrix} 5.9963 \\ 7.3965 \\ 18.141 \end{bmatrix} e_r \quad (55)$$

$$u = \begin{bmatrix} -8.4545 & -10.429 & -25.579 \end{bmatrix} \zeta - 5.6398 e_r, \quad (56)$$

³MATLAB function `h2hinfsyn` was used to synthesize the controller.

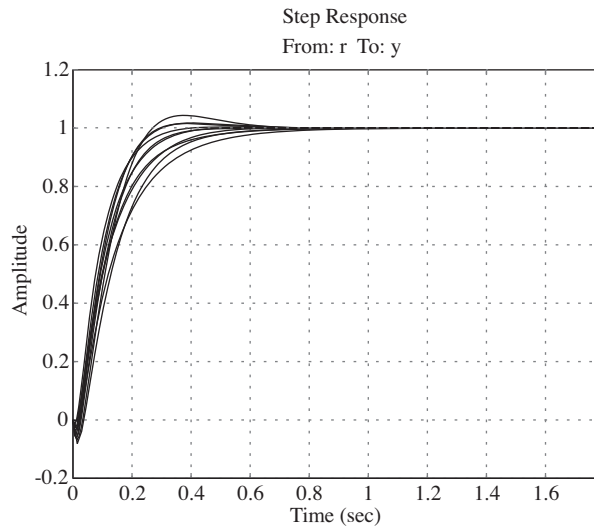


Figure 2. Step response of the closed-loop system from reference r to output y for ten random values of the parameter vector.

which archives a finite \mathcal{L}_2 gain $\gamma = 0.371$ from $\text{col}(e_d, r)$ to e_r for all $\hat{\theta}_L \in \Theta$. The controller can also be expressed in transfer function form as

$$K(s) = \frac{-5.6398 (s + 174.9)(s + 33.42)(s + 8.989)}{s(s + 19.74)(s + 92.58)}. \tag{57}$$

From the Galerkin system coefficients, the constants k_6 and k_7 were evaluated to be 34.85 and 16.11, respectively, and recalling that $k = 1000$ for the adaptation scheme, it can be verified that γ satisfies condition (34) of Theorem 5.1.

The next step is the verification that this controller performs satisfactorily for the entire parameter range Θ . Figure 2 shows the closed-loop step response of the system from the reference r to output y for ten random values of the parameter vector $\hat{\theta}_L$. It can be seen that the closed-loop system is successful in tracking the step reference in all cases. It is possible to show that the LPV system has an unstable zero for all $\hat{\theta}_L \in \Theta$, and hence the non-minimum phase behavior in the plot.

Figure 3 shows the closed-loop step response from the adaptation error e_d to the output y for ten random values of the parameter vector $\hat{\theta}_L$. Recall that the adaptation error $e_d := \text{col}\{e_1, e_2, e_3\}$ is regarded as a disturbance for the LPV system. It can be seen that the adaptation error does not interfere with the operation significantly since a step excitation from the e_d channel only effects the output at magnitudes of order 10^{-2} , which is acceptable.

As the next step in evaluation, feedback using the controller (57) is applied to the nonlinear Galerkin system. Figure 4 shows the error $e_d = \hat{a} - a$ between the states a of the Galerkin system (52)–(53) and the reconstructed states \hat{a} of the LPV system (48) under a step input signal. It can be seen that the magnitude of the error is quite small and less than 10^{-3} , which means that the LPV system approximates the nonlinear Galerkin system very closely through the parameter adaptation scheme (23).

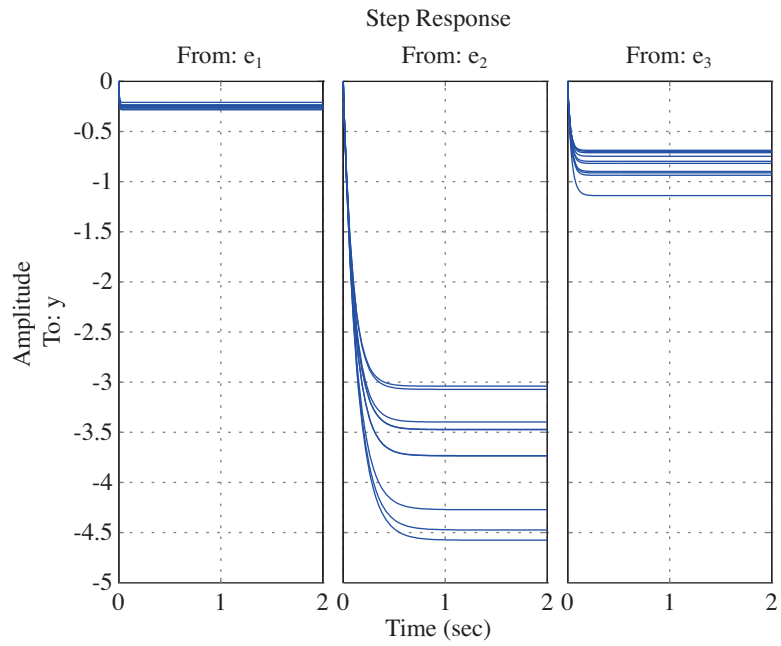


Figure 3. Step response of the closed-loop system from the adaptation error e_d to output y for ten random values of the parameter vector.

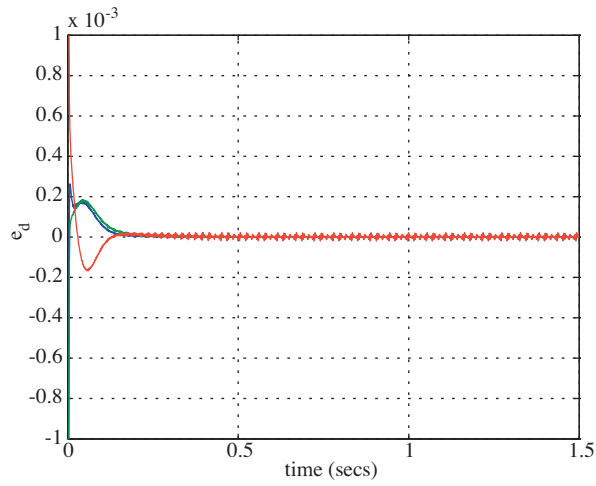


Figure 4. Error e_d between nonlinear Galerkin system states and reconstructed states in closed-loop under a step input.

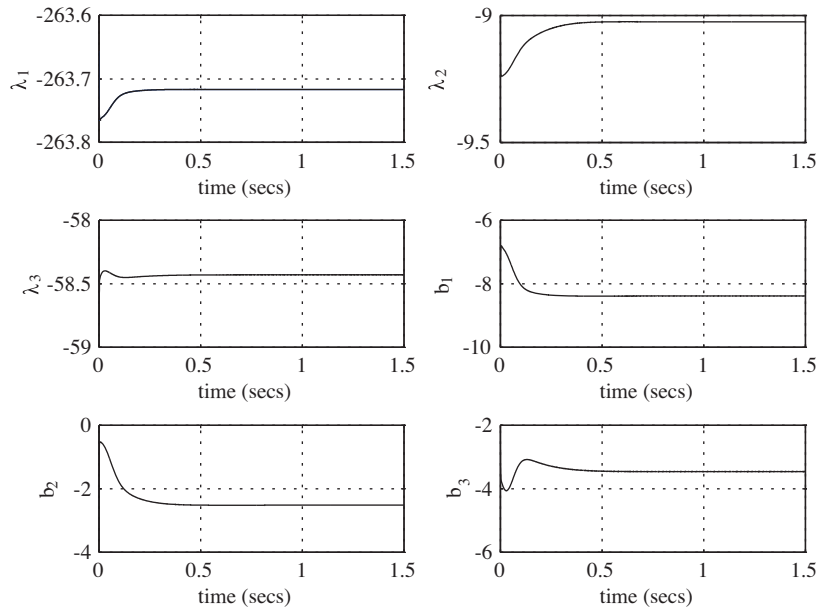


Figure 5. Parameter vector $\hat{\theta}_L$ produced by the adaptation mechanism during closed-loop operation under a step input.

Figure 5 shows the parameter values produced by this adaptation scheme, which are seen to lie well within the range Θ in (54) for which the closed-loop system was evaluated earlier.

Figure 6 shows the output of the nonlinear Galerkin system in closed-loop under a step input, which is seen to reach and settle to the desired reference value in less than one second.

The final step in the evaluation process is to connect the controller in feedback with the actual Navier-Stokes equations (39)–(40) and perform computational fluid dynamics (CFD) simulations to evaluate the performance of the closed-loop system. This step is crucial because the Galerkin system itself is an approximation of the flow dynamics. The actual flow dynamics can only be described accurately by the Navier-Stokes PDEs, on which direct analysis and design is not feasible due to their complexity. It is however possible and necessary to verify the controllers on these equations through numerical CFD simulations. For this purpose *Navier2D* solver under MATLAB [52] was utilized, with the reference signal r being a square wave alternating between 1 and -1 . Snapshots from the CFD simulation for this case are shown in Figures 14–15, and the system output y , the reference tracking error e_r , and the control input u are shown in Figure 16. It can be observed that the closed-loop system successfully tracks the given reference signal. The example illustrates that, under the guidance of Theorem 5.1, a controller design based on the approximate LPV model achieves the desired task when applied to the nonlinear Galerkin model and to the Navier Stokes PDEs.

7.5. Additional analysis

The LPV model and its parameter range Θ provided by the adaptation mechanism can also be used to obtain various robustness estimates of the closed-loop system, e.g. determining the sensitivity to input and output disturbances entering the plant. Figure 10 shows the step response and Figure 11 shows the frequency response of the closed-loop system to an input disturbance for ten random values of the parameter vector. The value of

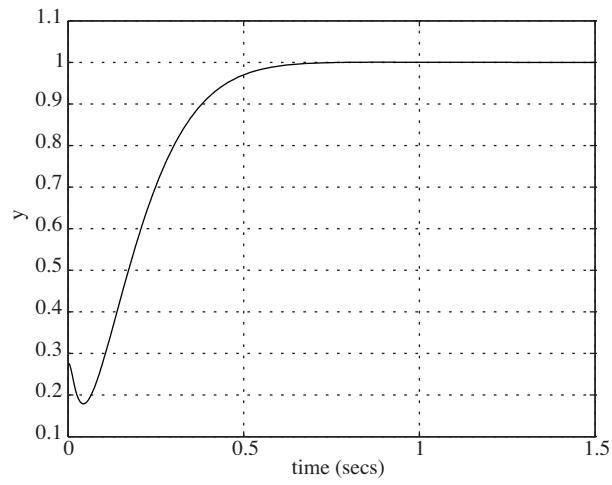


Figure 6. Nonlinear Galerkin system output in closed-loop under a step input.

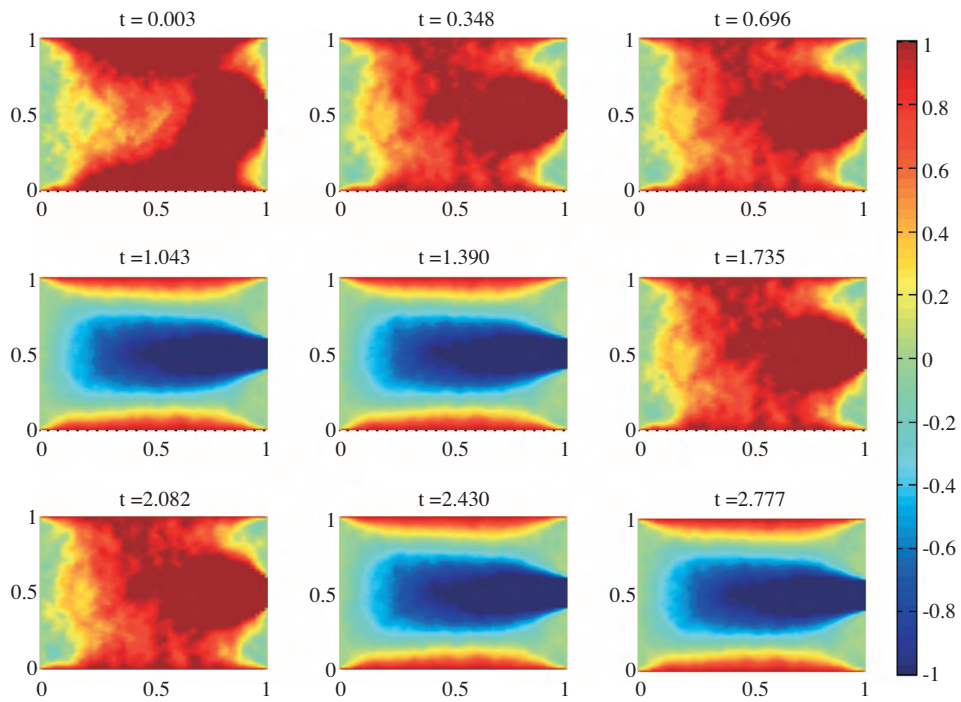


Figure 7. Snapshots (u -component) from the CFD simulation for the Navier-Stokes system under closed-loop.

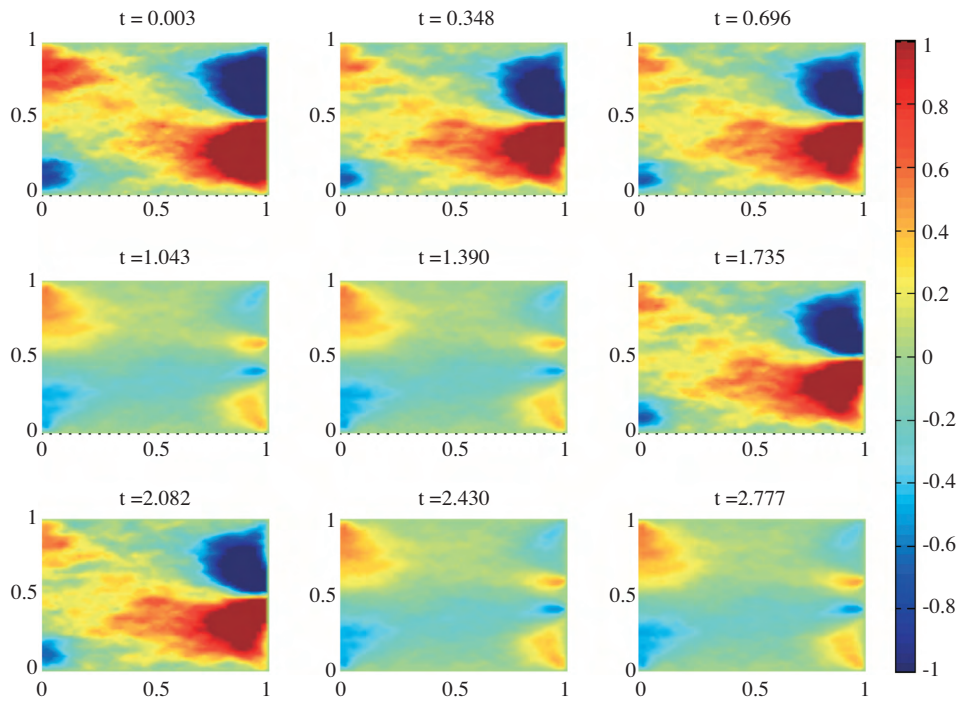


Figure 8. Snapshots (v -component) from the CFD simulation for the Navier-Stokes system under closed-loop.

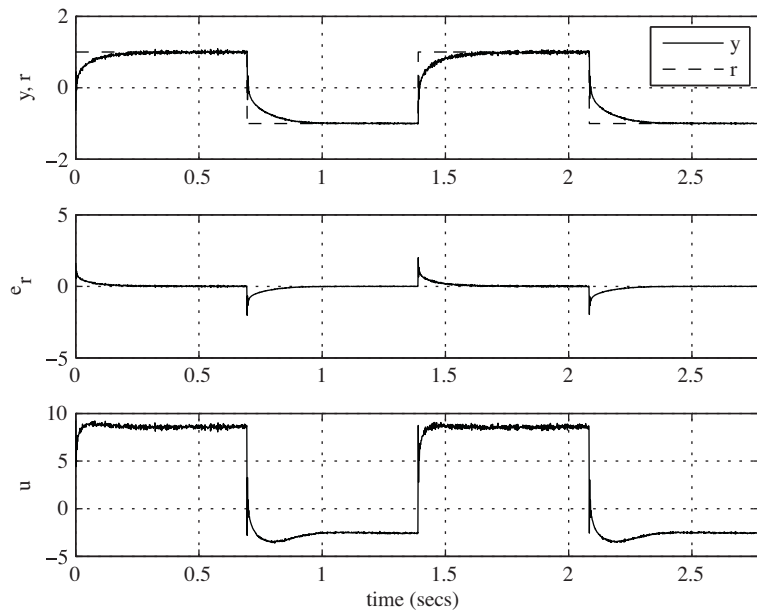


Figure 9. Point of interest (i.e. system output y), tracking error e_r and control signal u for the Navier-Stokes system under closed-loop.

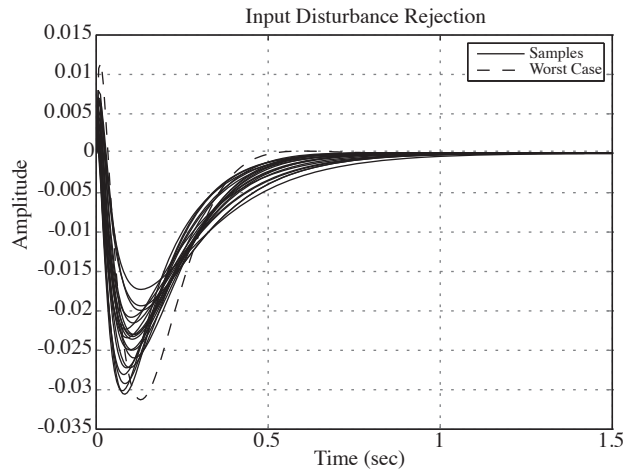


Figure 10. Response of the closed-loop system to a step input disturbance, for ten random values of the parameter vector.

the parameter vector yielding the highest peak in the frequency response and its corresponding step response are also shown with dashed lines in the figures. The figures indicate that the closed-loop system in general has good input disturbance rejection properties, but attention is required if input noise of high amplitude around 13.21 rad/s is expected, since its attenuation may be slow and may interfere with the command signal given from the controller.

As for sensitivity to output disturbance, Figure 12 shows the step response and Figure 13 shows the frequency response of the closed-loop system to an output disturbance for ten random values of the parameter vector. The value of the parameter vector yielding to the highest peak in the frequency response and its corresponding step response are also shown with dashed lines in the figures. It can be seen from Figure 12 that

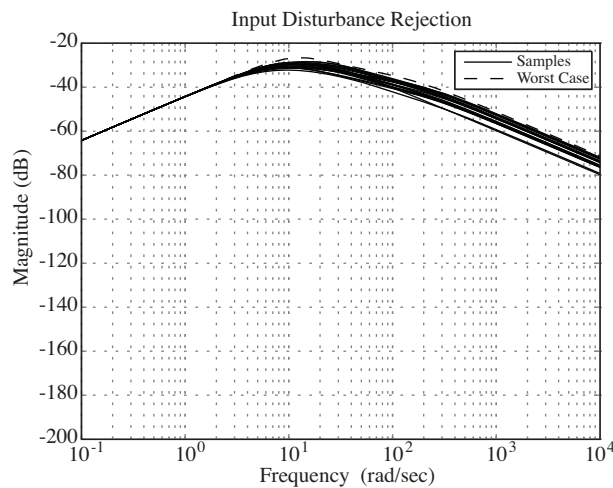


Figure 11. Frequency response of the closed-loop system to input disturbance, for ten random values of the parameter vector.

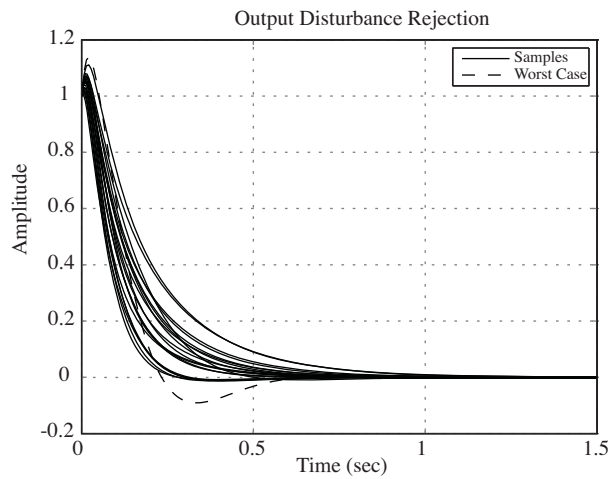


Figure 12. Response of the closed-loop system to a step output disturbance, for ten random values of the parameter vector.

the system in general is good at rejecting step disturbances. Looking at the frequency response in Figure 13, one sees that the system is sensitive to noise at the output at frequencies around 16.68 rad/s, and the gain to the output is around unity at higher frequencies. This is effect is somewhat expected, since the controller cannot differentiate what portion of the signal it receives is due to tracking error and what portion is due to output noise, and may erroneously try to follow a change due a noise signal. If this effect due to output noise is intolerable for the application at hand, one may try to make the output measurements less prone to noise (e.g. by insulation or by using better transducers), or perhaps filter the output for high frequencies if it can be assured that the reference signal will be slowly varying.

An additional type of robustness analysis that can be performed using the LPV model is to compute

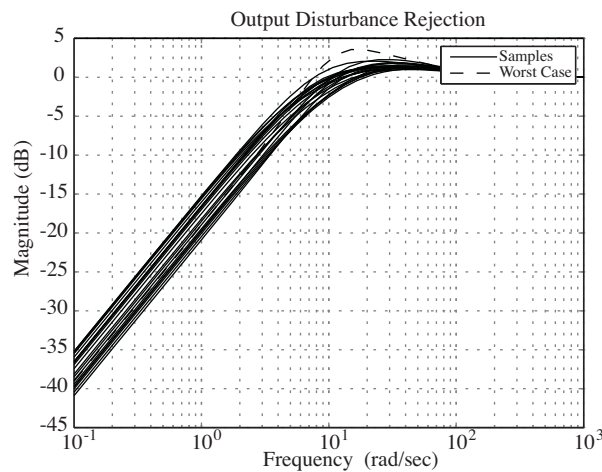


Figure 13. Frequency response of the closed-loop system to output disturbance, for ten random values of the parameter vector.

the robust stability margins of the closed-loop system. This analysis consists of verifying that the nominal system is stable and that no poles cross the stability boundary as the elements of the parameter vector $\hat{\theta}_L = [\hat{\lambda}_1 \hat{\lambda}_2 \hat{\lambda}_3 \hat{b}_1 \hat{b}_2 \hat{b}_3]^T$ are varied within their allowed range. By this analysis one can also gather information about the sensitivities with respect to individual elements of $\hat{\theta}_L$, i.e. which element affects stability the most. Carrying out a robust stability analysis using MATLAB function `robuststab` yields the following result:

```
Uncertain System is robustly stable to modeled uncertainty.
-- It can tolerate up to 131% of the modeled uncertainty.
-- A destabilizing combination of 534% of the modeled uncertainty exists,
    causing an instability at 39.6 rad/s.
-- Sensitivity with respect to uncertain element ...
' b1 ' is 19%. Increasing 'bb1u' by 25% leads to a 5% decrease in the margin.
' b2 ' is 29%. Increasing 'bb2u' by 25% leads to a 7% decrease in the margin.
' b3 ' is 16%. Increasing 'bb3u' by 25% leads to a 4% decrease in the margin.
' lambda1 ' is 25%. Increasing 'lambda1u' by 25% leads to a 6% decrease in the margin.
' lambda2 ' is 11%. Increasing 'lambda2u' by 25% leads to a 3% decrease in the margin.
' lambda3 ' is 5%. Increasing 'lambda3u' by 25% leads to a 1% decrease in the margin.
```

The analysis shows that the closed-loop system is robustly stable for all values of $\hat{\theta}_L \in \Theta$; in fact it is indicated that the closed-loop will remain stable for up to 114% of the specified uncertainty (i.e. the robust stability margin is 1.14). Among the individual elements of $\hat{\theta}_L$, the robust stability margin is most sensitive to variations in the element \hat{b}_2 and least sensitive to the variations in $\hat{\lambda}_3$.

START HERE /NEXT To verify the predictions based on the LPV models regarding input and output sensitivities, additional CFD simulations were performed in the presence of noises. For the first simulation an input noise of $0.5 \sin(13.21t)$ was applied to the system. Recall from Figure 11 that $\omega = 13.21$ rad/s is the frequency under which the frequency response peaks for the worst case. Snapshots for the CFD simulation for this case are shown in Figures 14–15 and the system output y , the reference tracking error e_r , and the control input u are shown in Figure 16. It can be observed that the results are consistent with predictions based on the LPV model, and the closed-loop system is successful in tracking the input reference, while at the same time significantly attenuating the effect of the input disturbance to the output.

For the second simulation, an output noise of $0.5 \sin(16.68t)$ was applied to the system. The snapshots for the CFD simulation for this case are shown in Figures 17–18 and the system output (42), i.e. the u -velocity at the center of the domain, tracking error e_r and control signal u are shown in Figure 19. Unlike the input noise case considered previously, the system is not very robust to the output disturbance and its effect occurs as an oscillation of amplitude about 0.16 around the reference to be tracked. This is also consistent with the earlier analysis based on the LPV model approximation, which had revealed that the closed-loop system is not very good at attenuating output disturbances, except for those at low frequencies. Hence, as suggested earlier, if significant noise is expected on the output measurements, and the reference command is known to be slowly varying, one might consider filtering out the high frequencies before the signal is fed into the controller.

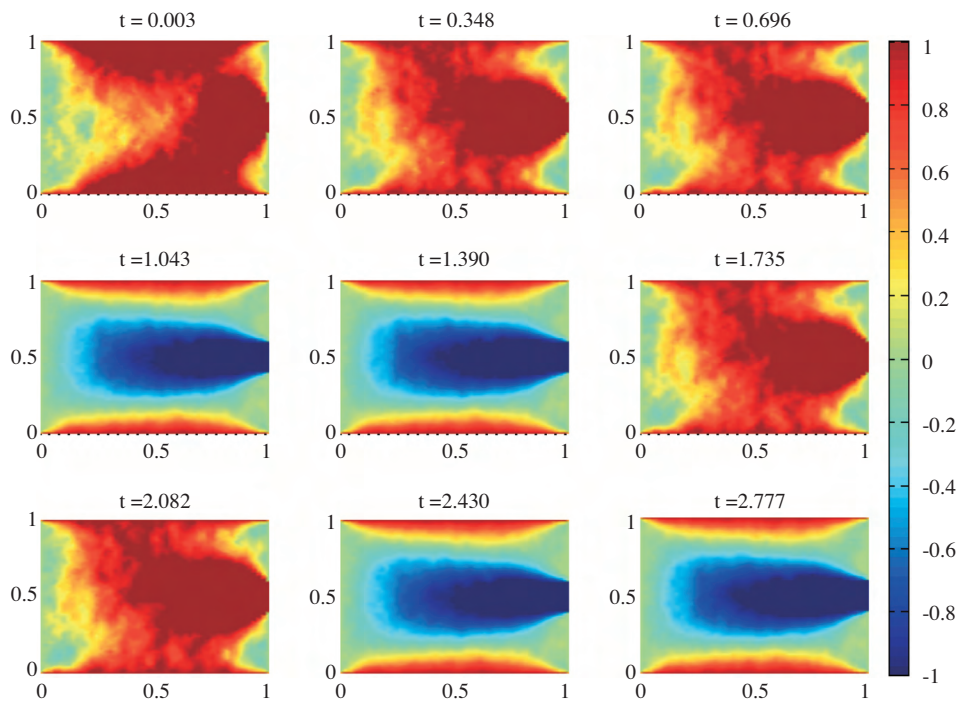


Figure 14. Snapshots (u-component) of CFD simulation for the Navier-Stokes system under closed-loop with input noise.

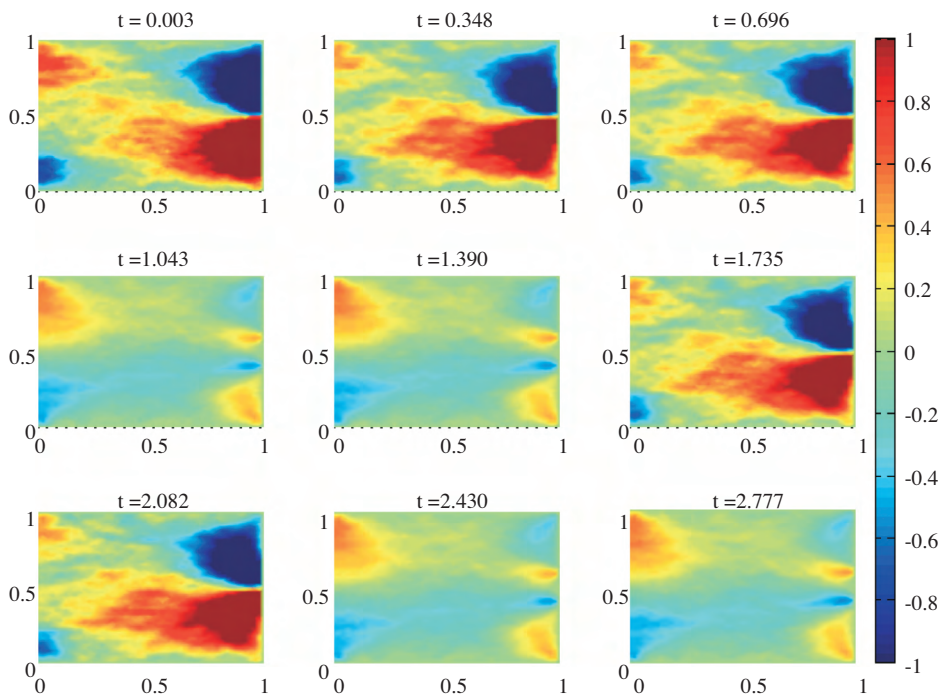


Figure 15. Snapshots (v-component) of CFD simulation for the Navier-Stokes system under closed-loop with input noise.

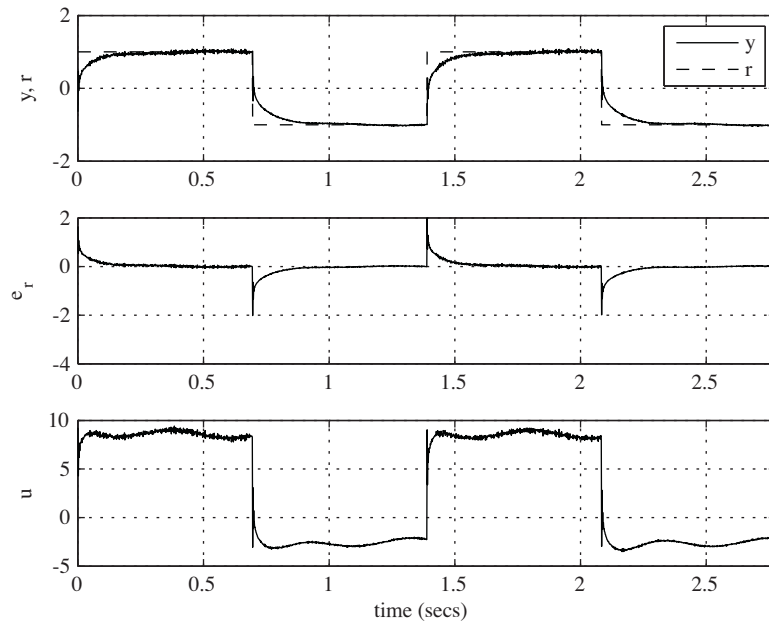


Figure 16. Point of interest (i.e. system output y), tracking error e_r and control signal u for the Navier-Stokes system under closed-loop with input noise.

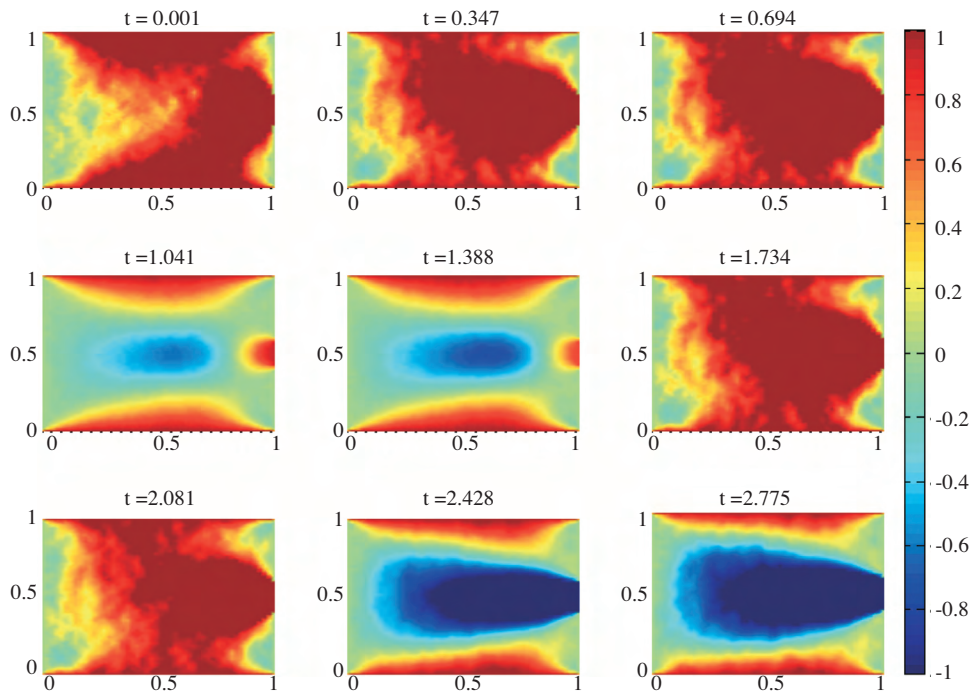


Figure 17. Snapshots (u -component) of CFD simulation for the Navier-Stokes system under closed-loop with output noise.

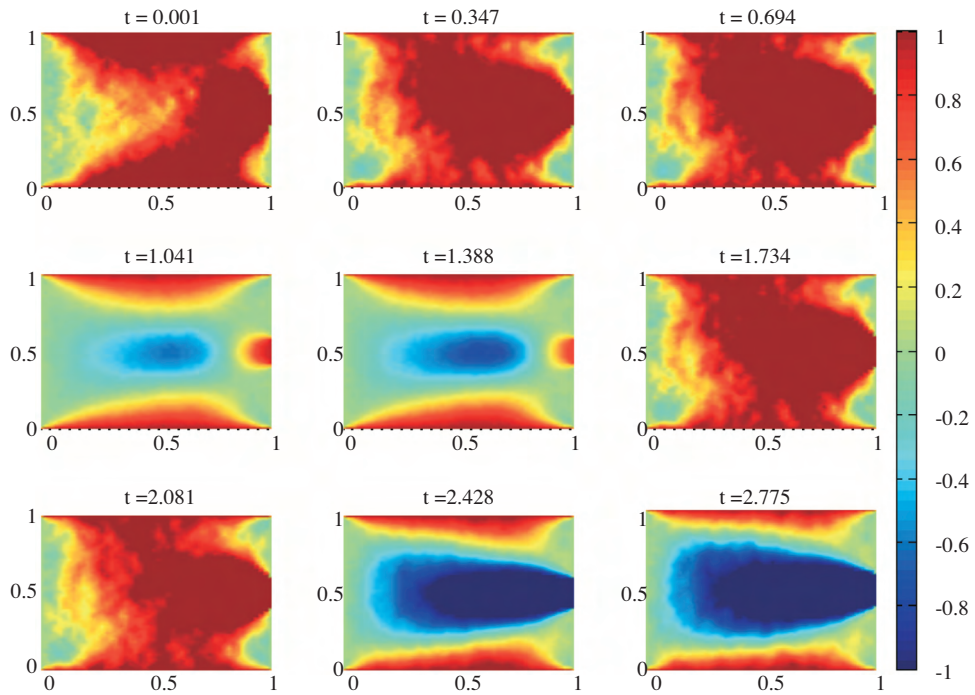


Figure 18. Snapshots (v -component) of CFD simulation for the Navier-Stokes system under closed-loop with output noise.

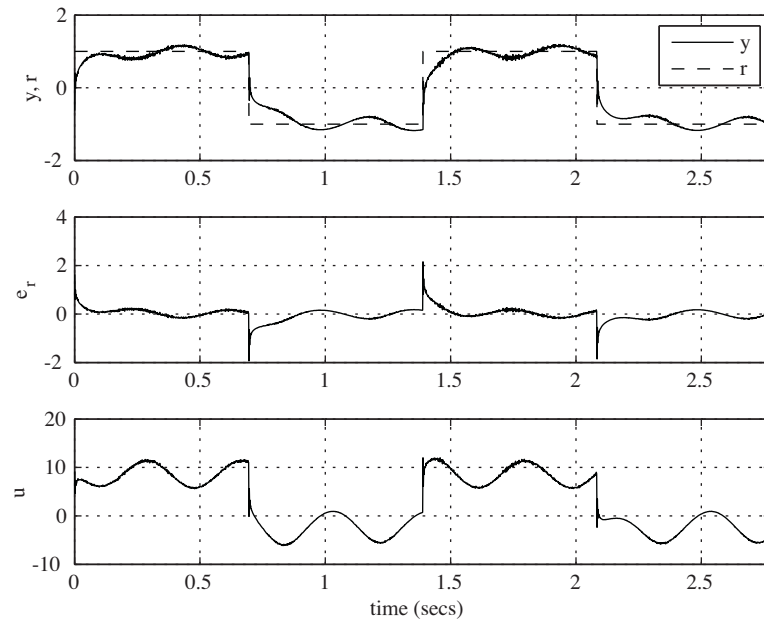


Figure 19. Point of interest (i.e. system output y), tracking error e_r and control signal u for the Navier-Stokes system under closed-loop with output noise.

8. Conclusions, discussions and future work

In this paper a systematic approach to the modeling and control of fluid flow problems is considered, which is based on building an LPV model whose parameter vector is governed by an adaptation mechanism. After POD/GP/IS techniques are applied to the fluid flow PDEs, the resulting nonlinear Galerkin model is approximated by an LPV model, where the approximation is achieved by varying the parameters of the LPV model through the adaptation scheme. Controller design can then be performed on the LPV model, instead of dealing with the nonlinear Galerkin model. One such controller design possibility is also explored, where an \mathcal{H}_∞ controller design is carried out on the LPV model and is subsequently applied to the nonlinear Galerkin model. It is shown that if certain conditions are satisfied, then the controller achieving the desired task on the LPV model will also succeed on the nonlinear Galerkin model.

The ideas of the paper are illustrated on a flow control example governed by the Navier-Stokes PDEs. It is seen from CFD simulations that the proposed modeling and control design approach achieves a desired regulation within the flow domain. In addition, it is demonstrated that the LPV model can be used to predict certain robustness properties of the closed-loop system.

The main contribution of this paper is to present a systematic and alternate methodology of dealing with flow control problems. The method allows for carrying out analysis and design tasks on an LPV model instead of a nonlinear model. This is advantageous since there are standard methods available for dealing with LPV systems, whereas nonlinear analysis and control design is much more difficult and case dependent.

We should point out that, as opposed to the mathematical approach presented in the paper, there exist physical methods in literature for approaching similar flow control problems. For instance, one can find techniques based on the decomposition of flow in low-frequency (base flow), dominant frequency (coherent structures), and high-frequency (small scale fluctuations) compartments [53, 54]. According to this strategy, the parameter to be adjusted are related to the amplitudes of the base-flow modes. It should also be mentioned that the LPV models may not be adequate in describing certain strong nonlinearities, whose exploitation might be advantageous in some cases for efficient turbulence control [55, 56].

Future research directions include employing alternative controller design methods to the LPV model and applying the results to additional flow control applications.

Acknowledgements

We would like to greatly acknowledge professors Mo Samimy, Andrea Serrani and all members of the OSU GDTL Flow Control Group for our collaborative works on cavity flow control, and also professors Bernd Noack and Gilead Tadmor for fruitful and insightful discussions during the initial phases of our research. We would also like to thank Darren Engwirda for providing the Navier-Stokes CFD Solver and answering our questions about it.

9. Appendices

A. Proof of Theorem 5.1

The proof relies on the concepts of dissipative systems and input-to-state stability (ISS) [57]. The closed loop system formed with the controller K (32)–(33) and system (29)–(30) is a linear system satisfying $\|\text{col}(e_d, r)\|_2 \leq \gamma \|r\|_2$ for all $\hat{\theta}_L \in \Theta$. Hence there exists a storage function $V_a = x_a^T X_{cl} x_a$ such that the closed-loop system is strictly dissipative with respect to the supply rate

$$q(e_d, r, e_r) = \gamma^2 \|\text{col}(e_d, r)\|^2 - \|e_r\|^2. \quad (58)$$

In other words,

$$\begin{aligned} \dot{V}_a(x_a) &\leq -\mu_a \|x_a\|^2 + q(e_d, r, e_r) = -\mu_a \|x_a\|^2 + \gamma^2 \|\text{col}(e_d, r)\|^2 - \|e_r\|^2 \\ &\leq -\mu_a \|x_a\|^2 + \gamma^2 \|e_d\|^2 + \gamma^2 \|r\|^2 - \|e_r\|^2 \end{aligned} \quad (59)$$

is satisfied for some $\mu_a \in \mathbb{R}_+$, where $x_a := \text{col}(\hat{a}, \zeta)$ is the augmented state vector containing the states of the LPV plant and the controller. Note that

$$\underline{\alpha}_a(\|x_a\|) \leq V_a(x_a) \leq \bar{\alpha}_a(\|x_a\|), \quad (60)$$

where $\underline{\alpha}_a(r) := \lambda_{\min} r^2$, $\bar{\alpha}_a(r) := \lambda_{\max} r^2$ and λ_{\min} , λ_{\max} are the smallest and largest eigenvalues of X_{cl} , respectively.

Let us also define

$$V_t(e_d, \hat{\theta}_L) := \frac{1}{2} \|\text{col}(e_d, \hat{\theta}_L)\|^2 = \frac{1}{2} e_d^T e_d + \frac{1}{2} \hat{\theta}_L^T \hat{\theta}_L. \quad (61)$$

Consider now the entire system including the LPV plant, controller, adaptation law and the nonlinear Galerkin model. Consider the state vector $x_e := \text{col}(\hat{a}, \zeta, e_d, \hat{\theta}_L)$ for the entire system. Note that the state of the Galerkin system is included implicitly since $a = \hat{a} - e_d$. Consider a candidate Lyapunov function

$$V(x_e) := V_a(\hat{a}, \zeta) + V_t(e_d, \hat{\theta}_L) \quad (62)$$

and note that

$$\underline{\alpha}_e(\|x_e\|) \leq V(x_e) \leq \bar{\alpha}_e(\|x_e\|), \quad (63)$$

where $\underline{\alpha}_e(r) = k_4 r^2$, $\bar{\alpha}_e(r) = k_5 r^2$ and

$$k_4 := \min\left\{\lambda_{\min}, \frac{1}{2}\right\} \quad (64)$$

$$k_5 := \max\left\{\lambda_{\max}, \frac{1}{2}\right\}. \quad (65)$$

Differentiating (62) along trajectories yields

$$\dot{V}(x_e) = \dot{V}_a(\hat{a}, \zeta) + \dot{V}_t(e_d, \hat{\theta}_L) \quad (66)$$

where we know that \dot{V}_a satisfies (59). To obtain a bound for \dot{V}_t , note from (61) that

$$\begin{aligned}
 \dot{V}_t &= e_d^T \dot{e}_d + \hat{\theta}_L^T \dot{\theta}_L \\
 &= e_d^T (\dot{\hat{a}} - \dot{a}) + \hat{\theta}_L^T \dot{\theta}_L \\
 &= e_d^T \left(\Phi_L(a, u) \theta_L - k e_d - \Phi_L(a, u) \theta_L - \Phi_N(a, u) \theta_N \right) \\
 &\quad + \hat{\theta}_L^T \left(-\Phi_L^T(a, u) e_d - \Upsilon(\hat{\theta}_L, a, u) - \Psi(\hat{\theta}_L) \right) \\
 &= e_d^T \Phi_L(a, u) \hat{\theta}_L - e_d^T k e_d - e_d^T (\Phi_L(a, u) \theta_L + \Phi_N(a, u) \theta_N) - \hat{\theta}_L^T \Phi_L^T(a, u) e_d \\
 &\quad - \hat{\theta}_L^T \hat{\theta}_L^* \|\text{col}(a, u)\|^4 - \hat{\theta}_L^T \hat{\theta}_L^* \|\text{col}(a, u)\|^2 - \hat{\theta}_L^T \Psi(\hat{\theta}_L) \\
 &= -k \|e_d\|^2 - e_d^T (L a + L_{\text{in}} u + Q(a, a) + Q_{\text{ain}}(a, u) + Q_{\text{in}}(u, u)) \\
 &\quad - \hat{\theta}_L^T \frac{\hat{\theta}_L}{\|\hat{\theta}_L\|^2} \|\text{col}(a, u)\|^4 - \hat{\theta}_L^T \frac{\hat{\theta}_L}{\|\hat{\theta}_L\|^2} \|\text{col}(a, u)\|^2 - \hat{\theta}_L^T \Psi(\hat{\theta}_L) \\
 &\leq -k \|e_d\|^2 + \|e_d\| \|L a + L_{\text{in}} u + Q(a, a) + Q_{\text{ain}}(a, u) + Q_{\text{in}}(u, u)\| - \|\text{col}(a, u)\|^4 \\
 &\quad - \|\text{col}(a, u)\|^2 - \hat{\theta}_L^T \Psi(\hat{\theta}_L) \\
 &\leq -k \|e_d\|^2 + \|e_d\| (\|L\| \|a\| + \|L_{\text{in}}\| \|u\| + \|Q\| \|a\|^2 + \|Q_{\text{ain}}\| \|a\| \|u\| + \|Q_{\text{in}}\| \|u\|^2) \\
 &\quad - \|\text{col}(a, u)\|^4 - \|\text{col}(a, u)\|^2 - \hat{\theta}_L^T \Psi(\hat{\theta}_L) \\
 &\leq -k \|e_d\|^2 + k_6 \|e_d\| \|\text{col}(a, u)\| + k_7 \|e_d\| \|\text{col}(a, u)\|^2 - \|\text{col}(a, u)\|^4 - \|\text{col}(a, u)\|^2 \\
 &\quad - \hat{\theta}_L^T \Psi(\hat{\theta}_L) \\
 &\leq -k \|e_d\|^2 + \frac{k_6^2}{2} \|e_d\|^2 + \frac{1}{2} \|\text{col}(a, u)\|^2 + \frac{k_7^2}{2} \|e_d\|^2 + \frac{1}{2} \|\text{col}(a, u)\|^4 - \|\text{col}(a, u)\|^4 \\
 &\quad - \|\text{col}(a, u)\|^2 - \hat{\theta}_L^T \Psi(\hat{\theta}_L),
 \end{aligned}$$

where

$$k_6 := \max\{\|L\|, \|L_{\text{in}}\|\} \quad (67)$$

$$k_7 := \max\{\|Q\| + \frac{1}{2}\|Q_{\text{ain}}\|, \|Q_{\text{in}}\| + \frac{1}{2}\|Q_{\text{ain}}\|\}, \quad (68)$$

and we have used Young's inequality⁴ as needed. Collecting similar terms,

$$\dot{V}_t \leq - \left(k - \frac{k_6^2}{2} - \frac{k_7^2}{2} \right) \|e_d\|^2 - \frac{1}{2} \|\text{col}(a, u)\|^2 - \frac{1}{2} \|\text{col}(a, u)\|^4 - \hat{\theta}_L^T \Psi(\hat{\theta}_L). \quad (69)$$

⁴Let $x, y, \varepsilon \in \mathbb{R}_+$, then $xy \leq \frac{x^2}{2\varepsilon} + \frac{\varepsilon y^2}{2}$.

Substituting (59) and (69) into (66) yields

$$\begin{aligned}
 \dot{V}(x_e) &= \dot{V}_a(\hat{a}, \zeta) + \dot{V}_t(e_d, \hat{\theta}_L) \\
 &\leq -\mu_a \|x_a\|^2 + \gamma^2 \|e_d\|^2 + \gamma^2 \|r\|^2 - \|e_r\|^2 - \left(k - \frac{k_6^2}{2} - \frac{k_7^2}{2}\right) \|e_d\|^2 - \frac{1}{2} \|\text{col}(a, u)\|^2 \\
 &\quad - \frac{1}{2} \|\text{col}(a, u)\|^4 - \hat{\theta}_L^T \Psi(\hat{\theta}_L) \\
 &\leq -\mu_a \|x_a\|^2 + \gamma^2 \|r\|^2 - \|e_r\|^2 - \left(k - \frac{k_6^2}{2} - \frac{k_7^2}{2} - \gamma^2\right) \|e_d\|^2 - \frac{1}{2} \|\text{col}(a, u)\|^2 \\
 &\quad - \frac{1}{2} \|\text{col}(a, u)\|^4 - \hat{\theta}_L^T \Psi(\hat{\theta}_L) \\
 &\leq \gamma^2 \|r\|^2 - \mu_a \|x_a\|^2 - \|e_r\|^2 - \left(k - \frac{k_6^2}{2} - \frac{k_7^2}{2} - \gamma^2\right) \|e_d\|^2 - k_\epsilon \|\hat{\theta}_L\|^2,
 \end{aligned} \tag{70}$$

where the last line follows from the fact that $-\Psi(\hat{\theta}_L) \leq -k_\epsilon \|\hat{\theta}_L\|$. Defining

$$k_8 := \min\{\mu_a, k - \frac{k_6^2}{2} - \frac{k_7^2}{2} - \gamma^2, k_\epsilon\}, \tag{71}$$

and using the fact that $-\|e_r\|^2 \leq 0$ yields

$$\dot{V}(x_e) \leq \gamma^2 \|r\|^2 - k_8 \|x_e\|^2. \tag{72}$$

Defining two class \mathcal{K}_∞ functions α and σ as

$$\alpha(s) := k_8 s^2 \tag{73}$$

$$\sigma(s) := \gamma^2 s^2, \tag{74}$$

and substituting into (72), yields

$$\dot{V}(x_e) \leq -\alpha(\|x_e\|) + \sigma(\|r\|), \tag{75}$$

which shows that the entire system is input-to-state stable (ISS) from input r to state $x_e = \text{col}(\hat{a}, \zeta, e_d, \hat{\theta}_L)$. This implies that there exists a class \mathcal{KL} function β and a class \mathcal{K} function Γ such that

$$\|x_e(t)\| \leq \beta(\|x_e(0)\|, t) + \Gamma(\|r\|_\infty). \tag{76}$$

The function Γ can be computed explicitly as ⁵

$$\Gamma(s) = \underline{\alpha}_e^{-1} \circ \bar{\alpha}_e \circ \alpha^{-1} k_9 \sigma(s) = \frac{k_5 k_9}{k_4 k_8} \gamma s, \tag{77}$$

where k_9 is any number greater than one. Hence for a bounded reference signal r , all state trajectories are bounded for all time. Also note from (70) that

$$\dot{V}(x_e) \leq \gamma^2 \|r\|^2 - \|e_r\|^2 \tag{78}$$

⁵See for instance [57], Remark 10.4.3.

which states that the system has finite \mathcal{L}_2 gain γ from r to e_r , i.e.

$$\|e_r\|_2 \leq \gamma \|r\|_2. \quad (79)$$

Similarly from (70) one can also write

$$\dot{V}(x_e) \leq \gamma^2 \|r\|^2 - \left(k - \frac{k_6^2}{2} - \frac{k_7^2}{2} - \gamma^2 \right) \|e_d\|^2, \quad (80)$$

which means that the system has finite gain finite \mathcal{L}_2 gain from r to e_r . In fact, it holds that

$$\|e_d\|_2 \leq \left(\frac{\gamma^2}{k - \frac{k_6^2}{2} - \frac{k_7^2}{2} - \gamma^2} \right)^{\frac{1}{2}} \|r\|_2, \quad (81)$$

which is the statement of the theorem. \square

B. Coefficients of the galerkin system for the example problem

The coefficients of the Galerkin system (11) for example studied in Section 7, namely the control of 2D incompressible Navier-Stokes flow on a square domain ,are as follows:

$$\begin{aligned} C_i &= \left\langle \begin{bmatrix} C_{i,u} \\ C_{i,v} \end{bmatrix}, \phi_i \right\rangle, \quad L_{ij} = \left\langle \begin{bmatrix} L_{ij,u} \\ L_{ij,v} \end{bmatrix}, \phi_i \right\rangle, \quad L_{in,i} = \left\langle \begin{bmatrix} L_{in,i,u} \\ L_{in,i,v} \end{bmatrix}, \phi_i \right\rangle, \\ Q_{ijk} &= \left\langle \begin{bmatrix} Q_{ijk,u} \\ Q_{ijk,v} \end{bmatrix}, \phi_i \right\rangle, \quad Q_{in,i} = \left\langle \begin{bmatrix} Q_{in,i,u} \\ Q_{in,i,v} \end{bmatrix}, \phi_i \right\rangle, \quad Q_{ain,ij} = \left\langle \begin{bmatrix} Q_{in,ij,u} \\ Q_{in,ij,v} \end{bmatrix}, \phi_i \right\rangle \end{aligned}$$

where

$$\begin{aligned} C_{i,u} &= -q_{0u} \frac{\partial}{\partial x} q_{0u} + Re^{-1} \left(\frac{\partial^2}{\partial x^2} q_{0u} + \frac{\partial^2}{\partial y^2} q_{0u} \right) - q_{0v} \frac{\partial}{\partial y} q_{0u} \\ C_{i,v} &= -q_{0u} \frac{\partial}{\partial x} q_{0v} + Re^{-1} \left(\frac{\partial^2}{\partial x^2} q_{0v} + \frac{\partial^2}{\partial y^2} q_{0v} \right) - q_{0v} \frac{\partial}{\partial y} q_{0v} \\ L_{ij,u} &= -(\phi_{u,j}) \frac{\partial}{\partial x} q_{0u} + Re^{-1} \left(\frac{\partial^2}{\partial x^2} (\phi_{u,j}) + \frac{\partial^2}{\partial y^2} (\phi_{u,j}) \right) - (\phi_{v,j}) \frac{\partial}{\partial y} q_{0u} \\ L_{ij,v} &= -(\phi_{u,j}) \frac{\partial}{\partial x} q_{0v} + Re^{-1} \left(\frac{\partial^2}{\partial x^2} (\phi_{v,j}) + \frac{\partial^2}{\partial y^2} (\phi_{v,j}) \right) - (\phi_{v,j}) \frac{\partial}{\partial y} q_{0v} \\ L_{in,i,u} &= -q_{0u} \frac{\partial}{\partial x} \psi_u - \psi_v \frac{\partial}{\partial y} q_{0u} + Re^{-1} \left(\frac{\partial^2}{\partial x^2} \psi_u + \frac{\partial^2}{\partial y^2} \psi_u \right) - \psi_u \frac{\partial}{\partial x} q_{0u} - q_{0v} \frac{\partial}{\partial y} \psi_u \\ L_{in,i,v} &= -q_{0u} \frac{\partial}{\partial x} \psi_v - \psi_v \frac{\partial}{\partial y} q_{0v} + Re^{-1} \left(\frac{\partial^2}{\partial x^2} \psi_v + \frac{\partial^2}{\partial y^2} \psi_v \right) - \psi_u \frac{\partial}{\partial x} q_{0v} - q_{0v} \frac{\partial}{\partial y} \psi_v \\ Q_{ijk,u} &= -(\phi_{u,k}) \frac{\partial}{\partial x} (\phi_{u,j}) - (\phi_{v,k}) \frac{\partial}{\partial y} (\phi_{u,j}) \\ Q_{ijk,v} &= -(\phi_{u,k}) \frac{\partial}{\partial x} (\phi_{v,j}) - (\phi_{v,k}) \frac{\partial}{\partial y} (\phi_{v,j}) \end{aligned}$$

$$Q_{in,i,u} = -\psi_v \frac{\partial}{\partial y} \psi_u - \psi_u \frac{\partial}{\partial x} \psi_v$$

$$Q_{in,i,v} = -\psi_v \frac{\partial}{\partial y} \psi_v - \psi_u \frac{\partial}{\partial x} \psi_v$$

$$Q_{in,ij,u} = -(\phi_{v,j}) \frac{\partial}{\partial y} \psi_u - (\phi_{u,j}) \frac{\partial}{\partial x} \psi_u - \psi_u \frac{\partial}{\partial x} (\phi_{u,j}) - \psi_v \frac{\partial}{\partial y} (\phi_{u,j})$$

$$Q_{in,ij,v} = -(\phi_{v,j}) \frac{\partial}{\partial y} \psi_v - (\phi_{u,j}) \frac{\partial}{\partial x} \psi_v - \psi_u \frac{\partial}{\partial x} (\phi_{v,j}) - \psi_v \frac{\partial}{\partial y} (\phi_{v,j}).$$

The reader interested in the details regarding the derivation of the Galerkin model and its coefficients above is referred to [34].

References

- [1] M. Gad-el Hak. *Flow Control: Passive, Active, and Reactive Flow Management*. Cambridge University Press, New York, NY, 2000.
- [2] T.R. Bewley. Flow control: new challenges for a new Renaissance. *Progress in Aerospace Sciences*, 37(1):21–58, 2001.
- [3] R.D. Joslin. Aircraft laminar flow control. *Annual review of fluid mechanics.*, 30:1–29, 1998.
- [4] Jiezhi Wu, Xiyun Lu, A.G. Denny, M. Fan, and J.M. Wu. Post-stall flow control on an airfoil by local unsteady forcing. *Journal of Fluid Mechanics*, 371:21–58, 1998.
- [5] O. M. Aamo, M. Krstic, and T. R. Bewley. Control of mixing by boundary feedback in 2d channel flow. *Automatica*, 39(9):1597–606–, 2003.
- [6] L. Baramov, O. R. Tutty, and E. Rogers. h_∞ control of non-periodic two-dimensional channel flow. *IEEE Transactions on Control Systems Technology*, 12(1):111–122, 2004.
- [7] L. Cortezzi, J. L. Speyer, K. H. Lee, and J. Kim. Robust reduced-order control of turbulent channel flows via distributed sensors and actuators. In *Proceedings of the 37th IEEE Conference on Decision and Control*, Tampa, FL, 1998.
- [8] M. Hogberg, T. R. Bewley, and D. S. Henningson. Linear feedback control and estimation of transition in plane channel flow. *Journal of Fluid Mechanics*, 481:149–175, 2001.
- [9] J. Kim. Control of turbulent boundary layers. *Physics of Fluids*, 15:1093, 2003.
- [10] A. Banaszuk, K. B. Ariyur, M. Krstic, and C. A. Jacobson. An adaptive algorithm for control of combustion instability. *Automatica*, 40(11):1965–72–, 2004.
- [11] K. Cohen, S. Siegel, T. McLaughlin, E. Gillies, and J. Myatt. Closed-loop approaches to control of a wake flow modeled by the Ginzburg-Landau equation. *Computers & Fluids*, 34(8):927–49–, 2005.
- [12] B. R. Noack and H. Eckelmann. A global stability analysis of the steady and periodic cylinder wake. *Journal of Fluid Mechanics*, 270:297–330, 1994.

- [13] B. R. Noack, K. Afanasiev, M. Morzynski, G. Tadmor, and F. Thiele. A hierarchy of low-dimensional models for the transient and post-transient cylinder wake. *Journal of Fluid Mechanics*, 497:335–63, 2003.
- [14] B. R. Noack, P. Papas, and P. A. Monkewitz. The need for a pressure-term representation in empirical Galerkin models of incompressible shear flows. *Journal of Fluid Mechanics*, 523:339–65, 2005.
- [15] C. W. Rowley, T. Colonius, and R. M. Murray. Model reduction for compressible flows using POD and Galerkin projection. *Physica D*, 189(1-2):115–29, 2004.
- [16] C. W. Rowley and J. E. Marsden. Reconstruction equations and the karhunen-loeve expansion for systems with symmetry. *Physica D*, 142(1-2):1–19, 2000.
- [17] K. Fitzpatrick, Y. Feng, R. Lind, A. J. Kurdila, and D. W. Mikolaitis. Flow control in a driven cavity incorporating excitation phase differential. *Journal of Guidance, Control, and Dynamics*, 28(1):63–70, 2005.
- [18] M. Samimy, M. Debiasi, E. Caraballo, A. Serrani, X. Yuan, J. Little, and J. H. Myatt. Feedback control of subsonic cavity flows using reduced-order models. *Journal of Fluid Mechanics*, 579:315–346, 2007.
- [19] E. Caraballo, J. Little, M. Debiasi, and M. Samimy. Development and implementation of an experimental based reduced-order model for feedback control of subsonic cavity flows. *Journal of Fluids Engineering*, 129:813–824, 2007.
- [20] W. R. Graham, J. Peraire, and K. Y. Tang. Optimal control of vortex shedding using low-order models. i - open-loop model development. *International Journal for Numerical Methods in Engineering*, 44:945–972, 1999.
- [21] S. N. Singh, J. H. Myatt, G. A. Addington, S. Banda, and J. K. Hall. Optimal feedback control of vortex shedding using proper orthogonal decomposition models. *Transactions of the ASME. Journal of Fluids Engineering*, 123(3):612–618, 2001.
- [22] K. Seiler, Z.H. Fan, K. Fluri, and D.J. Harrison. Electroosmotic Pumping and Valveless Control of Fluid Flow within a Manifold of Capillaries on a Glass Chip. *Analytical Chemistry*, 66(20):3485–3491, 1994.
- [23] R. Oleschuk, K. Westra, D.J. Harrison, A. Edmonton, and A. Microelectronic. Electrokinetic control of fluid flow in native poly (dimethylsiloxane) capillary electrophoresis devices. *Electrophoresis*, 21:107–115, 2000.
- [24] N. Smaoui. Boundary and distributed control of the viscous Burgers equation. *Journal of Computational and Applied Mathematics*, 182(1):91–104, 2005.
- [25] M. Hinze and K. Kunisch. Second order methods for boundary control of the instationary Navier-Stokes system. *Zeitschrift für Angewandte Mathematik und Mechanik*, 84(3):171–87, 2004.
- [26] T. Kobayashi and M. Oya. Nonlinear boundary control of coupled Burgers’ equations. *Control and Cybernetics*, 32(2):245–58, 2003.
- [27] H. M. Park and M. W. Lee. Boundary control of the Navier-Stokes equation by empirical reduction of modes. *Computer Methods in Applied Mechanics and Engineering*, 188(1-3):165–86, 2000.
- [28] M. Krstic. On global stabilization of Burgers’ equation by boundary control. *Systems & Control Letters*, 37(3):123–41, 1999.
- [29] P. Holmes, J.L. Lumley, and G. Berkooz. *Turbulence, Coherent Structures, Dynamical System, and Symmetry*. Cambridge University Press, Cambridge, 1996.

- [30] L. Sirovich. Turbulence and the dynamics of coherent structures. *Quarterly of Applied Math.*, XLV(3):561–590, 1987.
- [31] R Chris Camphouse. Boundary feedback control using Proper Orthogonal Decomposition models. *Journal of Guidance, Control, and Dynamics*, 28:931–938, 2005.
- [32] R. C. Camphouse. Actuator modes for reduced order modeling and boundary feedback control. Accepted to *Automatica*, 2007.
- [33] M. O. Efe and H. Ozbay. Low dimensional modelling and Dirichlet boundary controller design for Burgers equation. *International Journal of Control*, 77(10):895–906, July 2004.
- [34] C. Kasnakoglu, A. Serrani, and M. O. Efe. Control input separation by actuation mode expansion for flow control problems. *International Journal of Control*, 81(9):1475–1492, 2008. DOI: 10.1080/00207170701867857.
- [35] M.V. Kothare, B. Mettler, M. Morari, P. Bendotti, and C.M. Falinower. Linear parameter varying model predictive control for steam generator level control. *Computers and Chemical Engineering*, 21:861–866, 1997.
- [36] B.S. Hong, A. Ray, and V. Yang. Wide-range robust control of combustion instability. *Combustion and Flame*, 128(3):242–258, 2002.
- [37] G.J. Balas. Linear, parameter-varying control and its application to a turbofan engine. *International Journal of Robust and Nonlinear Control*, 12(9):763–796, 2002.
- [38] L. Giarré, D. Bauso, P. Falugi, and B. Bamieh. LPV model identification for gain scheduling control: An application to rotating stall and surge control problem. *Control Engineering Practice*, 14(4):351–361, 2006.
- [39] K. Fitzpatrick, Y. Feng, R. Lind, and A.J. Kurdila. Flow Control in a Driven Cavity Incorporating Excitation Phase Differential. *Journal of Guidance, Control, and Dynamics*, 28(1), 2005.
- [40] R. Lind. Linear parameter-varying modeling and control of structural dynamics with aerothermoelastic effects. *Journal of Guidance, Control, and Dynamics*, 25(4):733–739, 2002.
- [41] T. Sugiyama and K. Uchida. Gain-scheduled velocity and force controllers for electrohydraulic servo system. *Electrical Engineering in Japan*, 146(3):65–73, 2004.
- [42] M. Krstic, P.V. Kokotovic, and I. Kanellakopoulos. *Nonlinear and Adaptive Control Design*. John Wiley & Sons, Inc. New York, NY, USA, 1995.
- [43] K.J. Astrom and B. Wittenmark. *Adaptive Control*. Addison-Wesley Longman Publishing Co., Inc. Boston, MA, USA, 1994.
- [44] KS Narendra and AM Annaswamy. *Stable adaptive systems*. Prentice Hall Information and System Sciences Series, 1989.
- [45] J.J.E. Slotine and W. Li. *Applied nonlinear control*. Prentice Hall Englewood Cliffs, NJ, 1991.
- [46] C.P.A. Ioannou and J. Sun. *Robust Adaptive Control*. Prentice-Hall, Upper Saddle River, NJ, 1996.
- [47] C. Kasnakoglu, E. Caraballo, A. Serrani, and M. Samimy. Control input separation methods applied to cavity flow. In *27th American Control Conference*, Seattle, Washington, USA, 2008.

- [48] E. Caraballo, C. Kasnakoglu, A. Serrani, and M. Samimy. Control input separation methods for reduced-order model-based feedback flow control. *AIAA Journal*, 46(9):2306–2322, 2008.
- [49] K. Zhou, J.C. Doyle, and K. Glover. *Robust and optimal control*. Prentice Hall Upper Saddle River, NJ, 1996.
- [50] M. Chilali and P. Gahinet. H-infinity design with pole placement constraints: an LMI approach. *IEEE Transactions on Automatic Control*, 41(3):358–367, 1996.
- [51] P. Apkarian, P. Gahinet, and G. Becker. Self-Scheduled H-Infinity Control of Linear Parameter-Varying Systems—a Design Example. *Automatica*, 31(9):1251–1261, 1995.
- [52] D. Engwirda. An unstructured mesh navier-stokes solver. Master’s thesis, School of Engineering, University of Sydney, 2005.
- [53] B.R. Noack, M. Schlegel, B. Ahlborn, G. Mutschke, M. Morzynski, P. Comte, and G. Tadmor. A finite-time thermodynamics of unsteady fluid flows. *J. Non-Equilib. Thermodyn.*, 33(2):103–148, 2008.
- [54] B.R. Noack, M. Schlegel, M. Morzynski, and G. Tadmor. System reduction strategy for galerkin models of fluid flows. *Intl. J. Numer. Meth. Fluids*, 63(2), 2010.
- [55] D.M. Luchtenburg, B. Gunter, R. Noack, B.R. and King, and G. Tadmor. A generalized mean-field model of the natural and actuated flows around a high-lift configuration. *J. Fluid Mech.*, 623:283–316, 2009.
- [56] M. Pastoor, L. Henning, B.R. Noack, R. King, and G. Tadmor. Feedback shear layer control for bluff body drag reduction. *Journal of Fluid Mechanics*, 608:161–196, 2008.
- [57] A. Isidori. *Nonlinear Control Systems II*. Springer, London, UK, 1999.